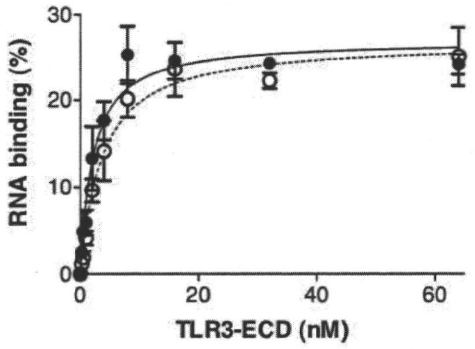

Figure 2. Binding curves of Family-I and -II aptamers for TLR3-ECD. Data points were obtained by a filter binding assay (50 μl reaction) as described in the Materials and Methods (Family-I, closed circles with solid line; Family-II, open circles with dotted line). The concentration of labeled aptamers was 1 nM. The values represent means of three independent experiments. RNA binding shows the percentage of RNA retained on the filter in protein/RNA complex against input RNA.

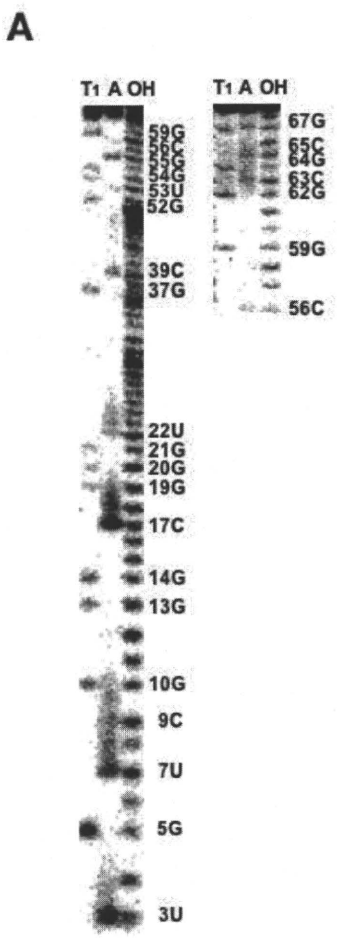

Figure 3. Enzymatic probing of Family-I and -II aptamers. 5'-end-labeled Family-I (A) and Family-II (C) aptamers were partially digested with RNase T1 (T1) or RNase A (A) and analyzed by 12% PAGE containing 7 M urea together with an alkaline ladder of them (OH). Nuclease-accessible sites in Family-I (B) and in Family-II (D) aptamers are shown by arrows (RNase T1) and open triangles (RNase A), respectively.

and pyrimidine nucleotides, respectively. 5'-end-labeled Family-I and -II RNAs were partially digested, and the cleavage products were analyzed by denaturing 12% PAGE (Fig. 3A and 3C). The secondary structures of the Family-I and -II aptamers, cleavage sites were observed mainly at unpaired residues, corresponding to loop regions and spacer sequences flanked by stem–loop structures (Fig. 3B and 3D). In general, the cleavage patterns of the two enzymes appear to be consistent with the proposed

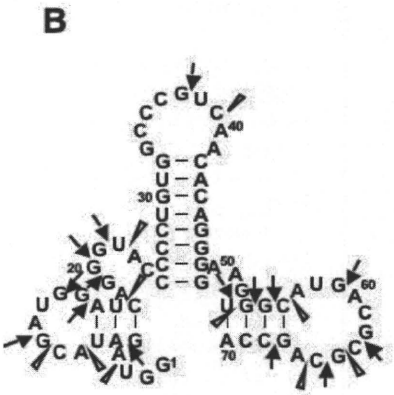

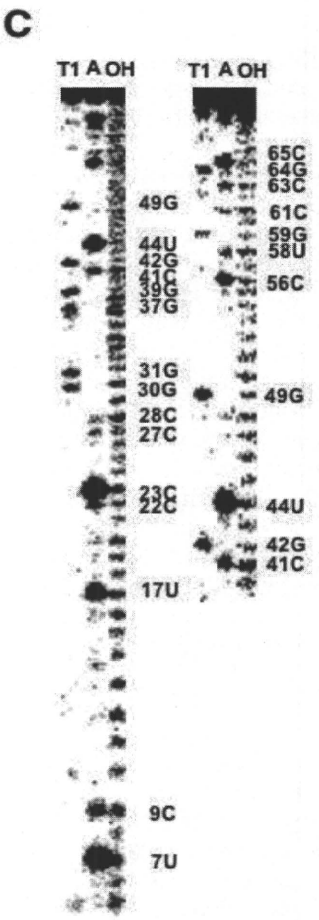

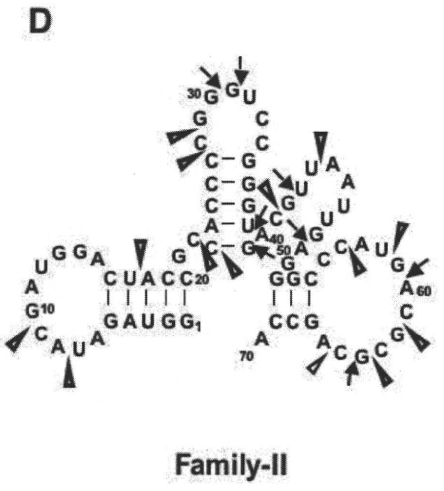

secondary structures of the Family-I and -II aptamers, which are composed of three stem–loop structures. Furthermore, sites that were not susceptible to cleavage were noted in the loop regions in both aptamers, suggesting that these loop structures might interact with other regions to form a tertiary structure, such as a pseudoknot. Taken together, these results provide experimental evidence to support the proposed secondary structures of Family-I and -II aptamers determined by the Mulfold program.

3.4. Structural and binding analyses of Family-I and -II aptamers

As mentioned above, no conserved sequence or structural similarity was observed between Family-I and -II aptamers (Fig. 1). To investigate the role of stem–loop structures in binding to TLR3-ECD, mutagenesis on Family-I and -II aptamers was carried out. Seven mutants were constructed in the Family-I aptamer sequence as follows (small letters indicate changed nucleotides): 1) dLoop I (ACGAUGG→ACGAU; GG at 3' end of Loop I deleted), 2) exStem I (two duplex sequences at Stem I interchanged), 3) mLoop II (GCCCGUCAA→GaaaGUCAA), 4) exStem II (several duplex sequences at Stem II interchanged), 5) dLoop III (AUGACGCGCA→aug; deletion of most of Loop III), 6) exStem III (two duplex sequence at Stem III interchanged), and 7) mSp I (AGGGUAC→AuuuUAC; the spacer sequence between SL I and SL II were mutated) (Fig. 4A).

The binding of ^{32}P-labeled mutant forms of Family-I aptamers to TLR3-ECD was examined by a filter binding assay as described in the Materials and Methods (Fig. 4B). We observed that the binding levels of dLoop I, exStem I, dLoop III, and exStem III, in which mutations were introduced into SL I and SL III, respectively, were almost comparable to that of wild type. However, mLoop II, exStem II, and mSpI dramatically lost the ability to bind to TLR3-ECD. These results suggest that in addition to the spacer sequence between SL I and SL II, the SL II structure in Family-I aptamers plays a significant role in binding to TLR3-ECD.

On the other hand, four mutants were constructed in the Family-II aptamer sequence as follows: 1) exStem I (three duplex sequences at Stem I interchanged), 2) mLoop II (CGGGUCC→CaaaUCC), 3) inStem II (several duplex sequences at Stem II inserted), and 4) mSp II (ACGUUAAUUGAG→ACGUaAAUaGAG; the spacer sequence between SL II and SL III was mutated) (Fig. 4C).

In a filter binding assay, exStem I retained binding ability as well as wild type (Fig. 4D). However, a drastic decrease of binding was observed in mLoop II, inStem II, and mSp II mutants (Fig. 4D). These results suggest that both SL II structure and the spacer sequence between SL II and SL III in Family-II aptamers are indispensable for binding to TLR3-ECD.

3.5. Selected aptamers have no effect on TLR3 signaling

To clarify the effect of Family-I and -II aptamers on TLR3 signaling, a reporter gene assay was performed as previously reported [21]. TLR3-negative HEK293 cells were transiently transfected with a human TLR3 expression plasmid, together with a reporter plasmid containing a luciferase gene under the control of the human IFN-β promoter; selected aptamers were then introduced into the cells. TLR3 preferentially recognizes poly(I:C) as an RNA ligand, therefore it was used as a positive control. Although TLR3-mediated IFN-β promoter activation by poly(I:C) was clearly observed, both Family-I and -II aptamers failed to induce luciferase gene expression (Fig. 5A). Next, we introduced both the selected aptamer and poly(I:C) into HEK293 cells in which TLR3 was transiently expressed to examine the competitive effect of Family-I and -II aptamers against poly(I:C) on TLR3 signaling. Although the competitive effects of Family-I and -II aptamers on the poly(I:C) induction were noticeable, the G0 RNA pool (N40H RNA pool) for the negative control also produced the same effect (Fig. 5B). Taken together, these selected aptamers showed neither agonistic, nor antagonistic effects in human TLR3-transfected HEK293 cells in spite of the high affinity binding to TLR3 ECD *in vitro*.

4. Discussion

TLR3 has an essential role in the innate immune response and recognizes polyinosinic-polycytidylic acid (poly(I:C)), a synthetic double-stranded (ds) RNA analog, as well as viral dsRNA, presumably formed during viral infection. The TLR3-mediated immune response induces the activation of NF-κB and the production of type I interferons, and thus TLR3 plays a key function in antiviral immune responses. On the other hand, several reports have shown that TLR3 does not display a protective function against some viral infections in spite of its anti-viral immune responses [8, 22]. Although poly(I:C), or a synthetic dsRNA analog, are potent inducers of TLR3 signaling, a

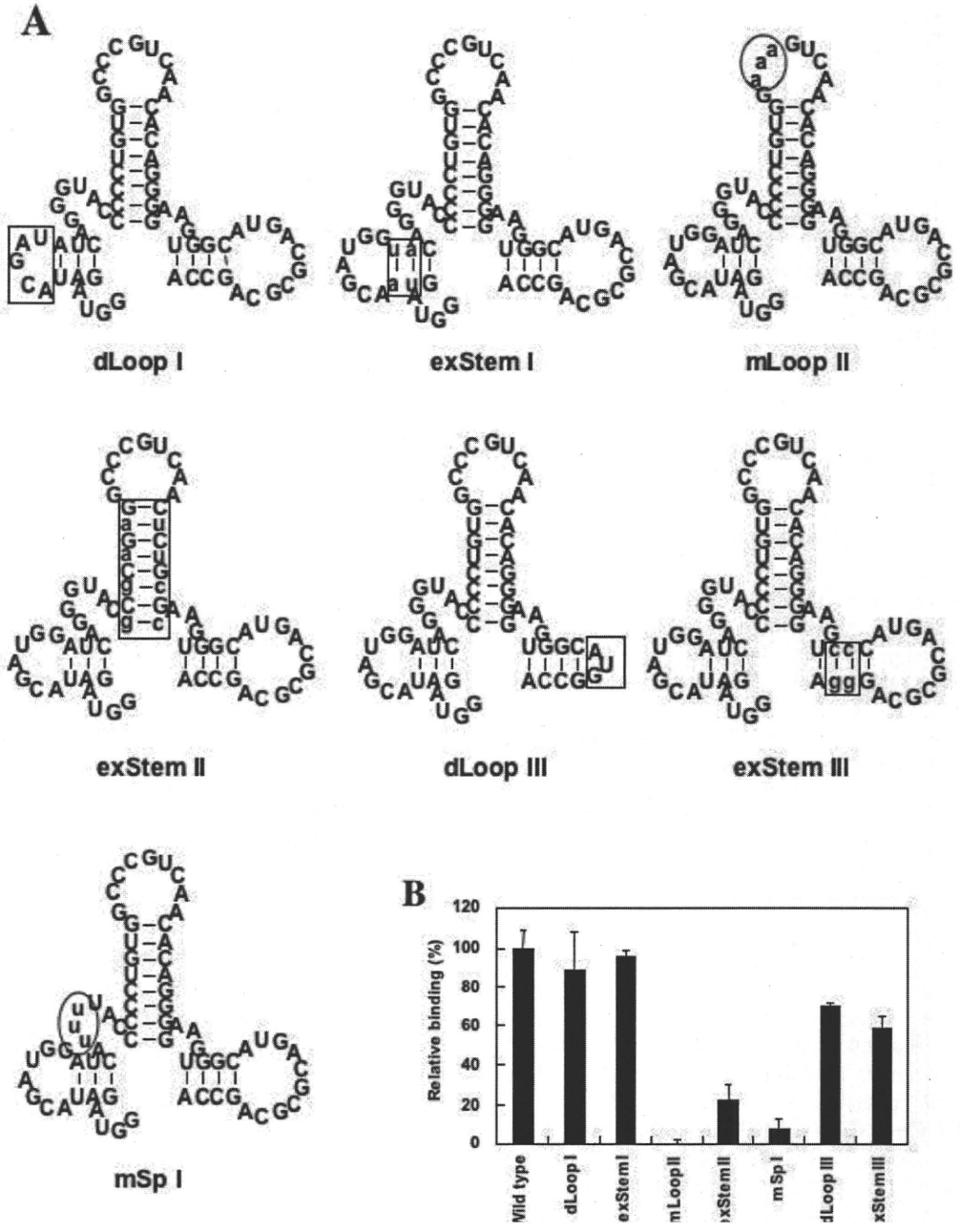

Figure 4. Binding analyses of Family-I and -II aptamer mutants to TLR3-ECD. Secondary structures of mutants in Family-I (A) and -II aptamers (C) are shown. Mutated regions are circled and boxed; small letters indicate the exchanged or introduced bases. The binding activity of Family-I (B) and -II (D) aptamer mutants were examined by a filter binding assay as described in the Materials and Methods. The values represent the means of three independent experiments and the relative RNA binding activity (wild type=100%) shows the percentage of RNA retained on the filter in protein/RNA complex against input RNA.

sequence-specific inducer, or inhibitor, has not been identified.

It is important to develop novel RNAs that function as anti-inflammatory drugs (TLR3 antagonists) and adjuvants for vaccines (TLR3 agonists). For this purpose, *in vitro* selection against TLR3 ECD was performed using a recombinant TLR3-ECD protein and a synthetic N40 random RNA pool. We succeeded in obtaining two classes of RNA aptamers specific for TLR3-ECD, designated as Family-I and -II. Although both show high affinity for the target with K_D values of about 2 to 4 nM, they do not harbor any conserved sequences between them. Mutational analyses on Family-I and -II aptamers revealed that particular regions, such as SL II structures and spacer sequences, are indispensable for binding to TLR3-ECD. The binding site of the selected RNA aptamers on TLR3 ECD is not known,

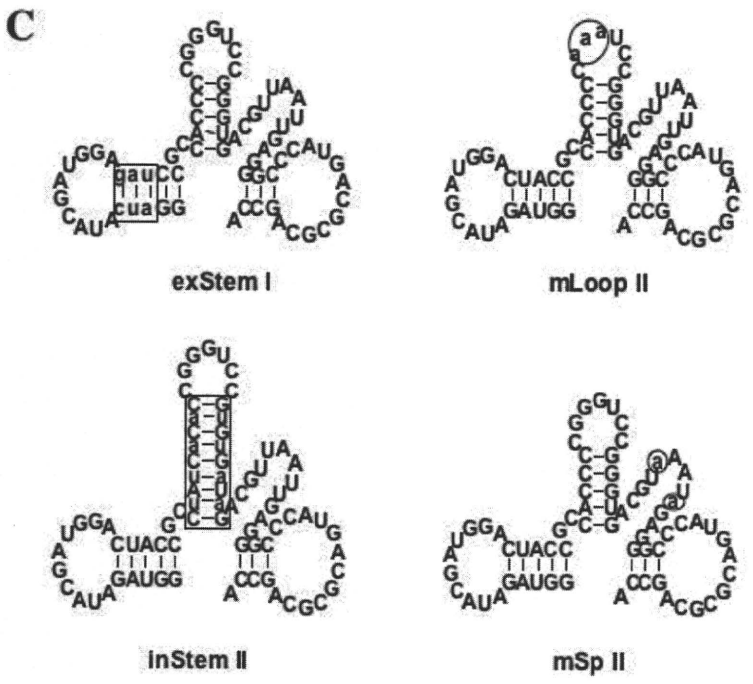

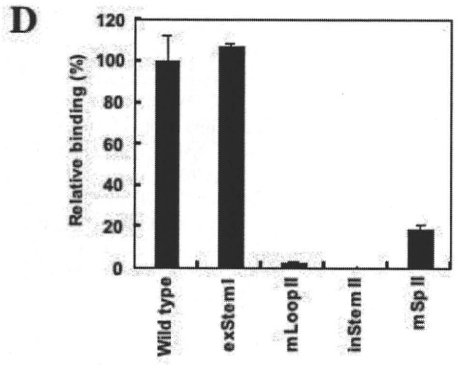

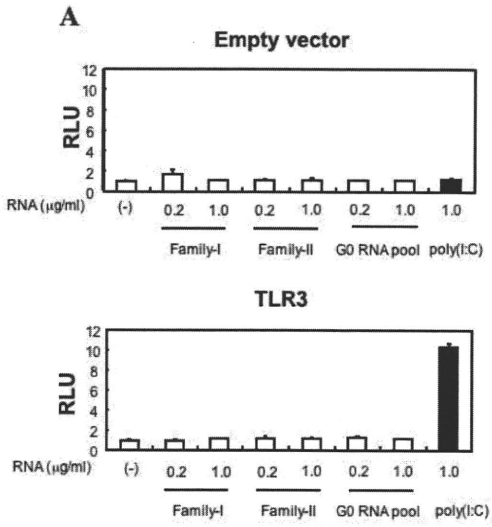

Figure 5. A reporter gene assay was carried out as described in the Materials and Methods. (A) HEK293 cells transfected with empty vector (pEF-BOS) or TLR3 expression vector (pEF-BOS/TLR3) were stimulated with Family-I and -II aptamers (0.2 and 1.0 μ g/ml), the G0 RNA pool (N40H RNA pool; 0.2 and 1.0 μ g/ml), or 1.0 μg/ml of poly(I:C) complexed with DOTAP. **(B)** Family-I and -II aptamers and the G0 RNA pool (2, 6, and 10 μg/ml) were introduced into HEK293 cells transfected with pEF-BOS or pEF-BOS/TLR3, in the presence, or absence, of 2 μg/ml of poly(I:C) complexed with DOTAP. The firefly luciferase activity was normalized to Renilla luciferase activity. Relative luciferase units (RLU) were calculated by dividing the normalized luciferase activity by the result obtained in the absence of RNA ligands (–).

although one possibility is that the two aptamers might interact with an electropositive region of the protein through ion pairs. Indeed, two patches, including several positively charged residues, are found on the glycosylation-free surface of TLR3 ECD [9, 10].

Two selected aptamers, which bind to TLR3-ECD with high affinity *in vitro*, had no influence on the TLR3 response. It has been reported that TLR3 localizes to acidic compartments and that acidic conditions are necessary for TLR3 signaling [12, 23]. Recent reports show that four highly conserved histidine residues, H39, H60, H108, and H539, that are protonated under acidic conditions, play a key role in recognizing dsRNA *in vitro* and *in vivo* [18, 24]. The RNA aptamers were isolated under neutral conditions; therefore we checked the binding ability of Family-I and –II under acidic conditions (pH 4.2) using a filter binding assay. From the results, both aptamers bound to TLR3-ECD as shown in the same experiment under neutral conditions (pH7.6) (data not shown). Furthermore, the G0 RNA pool, which was the non-selected initial RNA pool, also revealed the same binding behavior (data not shown). Taking into account all of these data, the specific interactions of the two aptamers may be diminished under acidic conditions due to the protonation of functional histidine residues in TLR3 ECD. This

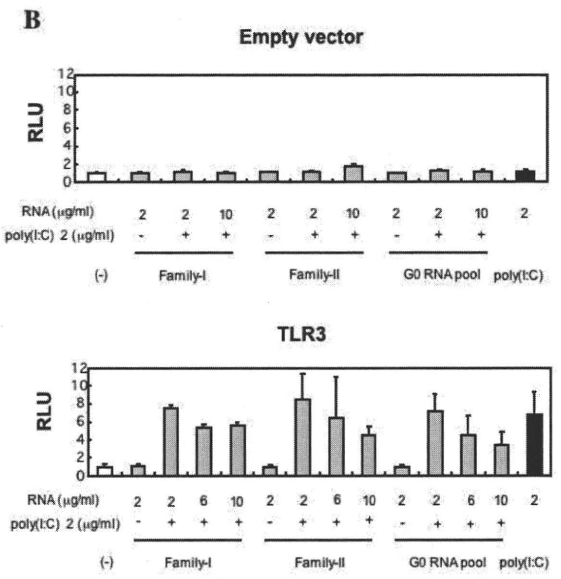

speculation is supported by the results, which showed that Family-I and –II aptamers mimicked the antagonistic effect as observed in the G0 RNA pool (Fig. 5B). In addition, the length of the double-stranded region of the RNA is also important for binding to TLR3 [21, 25]. Therefore, the binding region of the RNA aptamers may be too short, or their binding may not be specific to the functional regions of TLR3 ECD for proper signaling. Furthermore, steric hindrance by higher structure glycosylation, or the presence of co-receptors, or accessory molecules, may affect the precise interaction of ligands.

In this study, we obtained RNA aptamers (Family-I and -II) that bind to TLR3 ECD with high affinity. These aptamers showed neither agonistic, nor antagonistic effects on TLR3 signaling in a cell-based assay. However, the function of TLR3 might be manipulated by designing novel RNA constructs based on these two aptamers, or a new *in vitro* selection procedure under acidic conditions could create functional aptamers that regulate TLR3 signaling *in vivo*.

Acknowledgement
We thank T. Tokisue for helpful discussions.

References

1. Takeda, K., Kaisho, T., and Akira, S. Toll-like receptors, Annu. Rev. Immunol. 21, 335-376 (2003).
2. Gay, N. J., and Gangloff, M. Structure and function of Toll receptors and their ligands, Annu. Rev. Biochem. 76, 141-165 (2007).
3. Medzhitov, R. Toll-like receptors and innate immunity, Nat. Rev. Immunol. 1, 135-145 (2001).
4. O'Neill, L. A. TLRs: Professor Mechnikov, sit on your hat, Trends Immunol. 25, 687-693 (2004).
5. Akira, S., and Takeda, K. Toll-like receptor signaling, Nat. Rev. Immunol. 4, 499-511 (2004).
6. Alexopoulou, L., Holt, A. C., Medzhitov, R., and Flavell, R. A. Recognition of double-stranded RNA and activation of NF-kB by Toll-like receptor 3, Nature 413, 732-738 (2001).
7. Oshiumi, H., Matsumoto, M., Funami, K., Akazawa, T., and Seya, T. TICAM-1, an adaptor molecule that participates in Toll-like receptor 3-mediated interferon-β induction, Nat. Immunol. 4, 161-167 (2003).
8. Wang, T., Town, T., Alexopoulou, L., Anderson, J. F., Fikrig, E., and Flavell, R. A. Toll-like receptor 3 mediates West Nile virus entry into the brain causing lethal encephalitis, Nat. Med. 10, 1366-1373 (2004).
9. Choe, J., Kelker, M. S., and Wilson, I. A. Crystal structure of human Toll-like receptor 3 (TLR3) ectodomain, Science 309, 581-585 (2005).
10. Bell, J. K., Botos, I., Hall, P. R., Askins, J., Shiloach, J., Segal, D. M., and Davies, D. R. The molecular structure of the Toll-like receptor 3 ligand-binding domain, Proc. Natl. Acad. Sci. U. S. A. 102, 10976-10980 (2005).
11. Liu, L., Botos, I., Wang, Y., Leonard, J. N., Shiloach, J., Segal, D. M., and Davies, D. R. Structural basis of Toll-like receptor 3 signaling with double-stranded RNA, Science 320, 379-381 (2008).
12. Matsumoto, M., Funami, K., Tanabe, M., Oshiumi, H., Shingai, M., Seto, Y., Yamamoto, A., and Seya, T. Subcellular localization of Toll-like receptor 3 in human dendritic cells, J. Immunol. 171, 3154-3162 (2003).
13. Kawai, T., and Akira, S. Antiviral signaling through pattern recognition receptors, J. Biochem. 141, 137-145 (2007).
14. Marques, J. T., and Williams, B. R. Activation of the mammalian immune system by siRNAs, Nat. biotechnol. 23, 1399-1405 (2005).
15. Ellington, A. D., and Szostak, J. W. *In vitro* selection of RNA molecules that bind specific ligands, Nature 346, 818–822 (1990).
16. Tuerk, C., and Gold, L. Systematic evolution of ligands by exponential enrichment: RNA ligands to bacteriophage T4 DNA polymerase, Science 249, 505–510 (1990).
17. Tuerk, C. Using the SELEX combinatorial chemistry process to find high affinity nucleic acid ligands to target molecules, Methods Mol. Biol. 67, 219–230 (1997).
18. Fukuda, K., Watanabe, T., Tokisue, T., Tsujita, T., Nishikawa, S., Hasegawa, T., Seya, T., and Matsumoto, M. Modulation of double-stranded RNA recognition by the N-terminal histidine-rich region of the human Toll-like receptor 3, J. Biol. Chem. 283, 22787-22794 (2008).
19. Fukuda, K., Vishnuvardhan, D., Sekiya, S., Hwang, J., Kakiuchi, N., Taira, K., Shimotohno, K., Kumar, P. K., and Nishikawa, S. Isolation and characterization of RNA aptamers specific for the hepatitis C virus nonstructural protein 3 protease, Eur. J. Biochem. 267, 3685–3694 (2000).
20. Zuker, M. Computer prediction of RNA structure, Methods Enzumol. 180, 262-288 (1989).
21. Okahira, S., Nishikawa, F., Nishikawa, S., Akazawa, T., Seya, T., and Matsumoto, M. Interferon-b induction through Toll-like receptor 3 depends on double-stranded RNA structure, DNA Cell Biol. 24, 614-623 (2005).
22. Matsumoto, M., and Seya, T. TLR3: interferon induction by double-stranded RNA including poly(I:C), Advanced Drug Delivery Reviews 60, 805-812 (2008).
23. de Bouteiller, O., Merck, E., Hasan, U. A., Hubac, S., Benguigui, B., Trinchieri, G., Bates, E. E., and Caux, C. Recognition of double-stranded RNA by human Toll-like receptor 3 and downstream receptor signaling requires multimerization and an acidic pH, J. Biol. Chem. 280, 38133-38145 (2005).
24. Bell, J. K., Askins, J., Hall, P. R., Davies, D. R., and Segal, D. M. The dsRNA binding site of human Toll-like receptor 3, Proc. Natl. Acad. Sci. U. S. A. 103, 8792-8797 (2006).
25. Leonard, J. N., Ghirlando, R., Askins, J., Bell, J. K., Margulies, D. H., Davies, D. R., and Segal, D. M. The TLR3 signaling complex forms by cooperative receptor dimerization, Proc. Natl. Acad. Sci. U. S. A. 105, 258-263 (2008).

Published August 31, 2009

JEM

BRIEF DEFINITIVE REPORT

Epstein-Barr virus (EBV)–encoded small RNA is released from EBV-infected cells and activates signaling from toll-like receptor 3

Dai Iwakiri,[1] Li Zhou,[1] Mrinal Samanta,[1] Misako Matsumoto,[2] Takashi Ebihara,[2] Tsukasa Seya,[2] Shosuke Imai,[3] Mikiya Fujieda,[4] Keisei Kawa,[5] and Kenzo Takada[1]

[1]Department of Tumor Virology, Institute for Genetic Medicine, Hokkaido University, Sapporo 060-0815, Japan
[2]Department of Microbiology and Immunology, Hokkaido University Graduate School of Medicine, Sapporo 060-8638, Japan
[3]Department of Microbiology and [4]Department of Pediatrics, Kochi Medical School, Kochi University, Nangoku 783-8505, Japan
[5]Osaka Medical Center and Research Institute for Maternal and Child Health, Izumi 594-1101, Japan

Epstein-Barr virus–encoded small RNA (EBER) is nonpolyadenylated, noncoding RNA that forms stem-loop structure by intermolecular base-pairing, giving rise to double-stranded RNA (dsRNA)–like molecules, and exists abundantly in EBV-infected cells. Here, we report that EBER induces signaling from the Toll-like receptor 3 (TLR3), which is a sensor of viral double-stranded RNA (dsRNA) and induces type I IFN and proinflammatory cytokines. A substantial amount of EBER, which was sufficient to induce signaling from TLR3, was released from EBV-infected cells, and the majority of the released EBER existed as a complex with a cellular EBER-binding protein La, suggesting that EBER was released from the cells by active secretion of La. Sera from patients with infectious mononucleosis (IM), chronic active EBV infection (CAEBV), and EBV-associated hemophagocytic lymphohistiocytosis (EBV-HLH), whose general symptoms are caused by proinflammatory cytokines contained EBER, and addition of RNA purified from the sera into culture medium induced signaling from TLR3 in EBV-transformed lymphocytes and peripheral mononuclear cells. Furthermore, DCs treated with EBER showed mature phenotype and antigen presentation capacity. These findings suggest that EBER, which is released from EBV-infected cells, is responsible for immune activation by EBV, inducing type I IFN and proinflammatory cytokines. EBER-induced activation of innate immunity would account for immunopathologic diseases caused by active EBV infection.

CORRESPONDENCE
Kenzo Takada:
kentaka@igm.hokudai.ac.jp

Abbreviations used: CAEBV, chronic active EBV infection; dsRNA, double-stranded RNA; EBER, EBV-encoded small RNA; EBV-HLH, EBV-associated hemophagocytic lymphohistiocytosis; IM, infectious mononucleosis; IRF, IFN-regulatory factor; La, lupus erythematosis-associated antigen; LCL, lymphoblastoid cell line; PKR, RNA-activated protein kinase; RIG-I, retinoic acid–inducible gene-I; TLR, Toll-like receptor.

Epstein-Barr virus (EBV) is a ubiquitous human herpesvirus that infects >90% of the population. Primary EBV infection is generally asymptomatic; however, when the infection is delayed until adolescence or later, ~50% of cases manifest as infectious mononucleosis (IM). IM is characterized by the expansion of reactive T cells and is most likely to be an immunopathologic disease whose general symptoms are caused by proinflammatory cytokines, such as IL-1, IFN-γ, and TNF (Rickinson and Kieff, 2001). Chronic active EBV infection (CAEBV) and EBV-associated hemophagocytic lymphohistiocytosis (EBV-HLH) are also active EBV infections with persistent or recurrent IM-like symptoms. EBV-HLH is characterized by an EBV infection in T cells and the systemic release of proinflammatory cytokines, which subsequently causes hemophagocytosis of blood cells through the activation of macrophages (Kikuta et al., 1993; Rickinson and Kieff, 2001).

The EBV noncoding RNAs, EBV-encoded RNA 1 (EBER1) and EBER2, are 167 and 172 nt long, respectively, and are expected to form dsRNA-like structures (Rosa et al., 1981). EBER is the most abundant viral transcript in latently EBV-infected cells (Rymo, 1979), and binds to several cellular proteins including

S. Imai's present address is Sapporo Toho Hospital, Sapporo 065-0017, Japan.

The Rockefeller University Press $30.00
J. Exp. Med.
www.jem.org/cgi/doi/10.1084/jem.20081761

Published August 31, 2009

RNA-activated protein kinase (PKR; Clarke et al., 1991), ribosomal protein 22 (L22; Toczyski et al., 1994), lupus erythematosis–associated antigen (La; Lerner et al., 1981), and retinoic acid–inducible gene I (RIG-I; Samanta et al., 2006).

Here, we report that EBER exists in the sera of patients with active EBV infections and induces type I IFN and inflammatory cytokines through TLR3-mediated signaling. This may account for the pathogenesis of active EBV infections that are characterized by cytokinemia.

RESULTS AND DISCUSSION

EBER is present in the culture supernatants of EBV-infected cells

RT-PCR assays have revealed that EBER is present in the culture supernatants of the Burkitt's lymphoma–derived EBV-positive cell lines Mutu+ (Gregory et al., 1990) and Akata+ (Takada, 1984), and the EBV-transformed lymphoblastoid cell lines (LCLs). EBER was detected on day 1 of the culture, and its expression peaked on day 4 (Fig. 1 A). In a real-time PCR assay, 15–35 ng/ml EBER1 was released into the culture supernatants, whereas EBER2 was only faintly detected (Fig. 1 B).

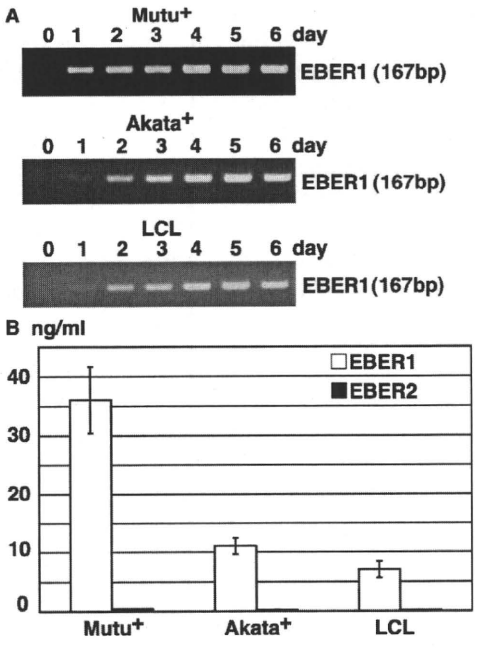

Figure 1. EBER1 is released into the culture supernatants of EBV-infected Mutu+, Akata+ and LCL. (A) RT-PCR of EBER1. Cells (2×10^5 cells/ml) were cultured for the designated number of days. Total RNA was extracted from 1 ml culture supernatant and subjected to 25 cycles of RT-PCR to detect EBER1. Three or more independent experiments were performed. (B) Quantitative RT-PCR of EBER1 and EBER2. Cells (2×10^5) were cultured in 1 ml medium for 4 d, and total RNA was extracted from the culture supernatant and subjected to RT-RCR for the detection of EBER1 and EBER2. Error bars indicate the SD of duplicate wells. The data presented are representative of three independent experiments.

EBER1 induces signaling from TLR3

To investigate the role of the EBER1 that was released from EBV-infected cells, we first examined whether in vitro–synthesized EBER1 could induce signaling from TLR3. RT-PCR assays indicated that LCLs and gastric carcinoma–derived NU-GC-3 cells (Akiyama et al., 1988) expressed TLR3 (Fig. 2 A).The addition of in vitro–synthesized EBER1 into culture medium induced IFN-β in LCLs and EBV-positive and -negative NU-GC-3 cells (Fig. 2 B; Imai et al., 1998). A similar result was also obtained by the TLR3 agonist poly(I:C). An ELISA indicated that IFN-β production was dependent on the amount of EBER1 that was added to the culture supernatants; we found that 0.1 ng/ml EBER1 was sufficient to induce the release of IFN-β (Fig. 2 C). Next, we evaluated the efficiency of EBER1 to induce IFN-β expression in LCLs comparing with poly(I:C). No difference in efficiency was observed between EBER1 and poly(I:C) by RT-PCR (Fig. 2 D).

When LCLs were pretreated with an anti-TLR3 antibody (Matsumoto et al., 2002), and then treated with EBER1, the effect of EBER1 on the induction of IFN-β was markedly reduced (Fig. 2 E). In addition, TLR3 knockdown by siRNA resulted in reduced induction of IFN (Fig. 2 F), indicating that EBER1 induces IFN through TLR3. IFN-regulatory factor 3 (IRF3) and NF-κB function downstream of the TLR3 signaling pathway (Akira and Takeda, 2004). As shown in Fig. 2 G, both IRF3 and NF-κB were phosphorylated upon treatment of the cells with EBER1 or poly(I:C).

We next examined whether the EBER1 that was released into culture supernatants could induce the expression of IFN. Cell culture supernatant was harvested on day 4 and added to the culture medium of LCLs. After 14 h of cultivation, the induction of IFN-β in LCLs was determined by RT-PCR. The results indicated that IFN was induced in EBV-positive cells, but not in EBV-negative cells or EBER-knockout EBV-infected cells (Fig. 2 H).

EBER1 is detected as a complex with La in the culture supernatants, and the complex can induce TLR3 signaling

The stable presence of EBER1 in culture supernatants suggested that EBER1 was bound by some proteins, thus being protected from degradation by nucleases. We then examined whether the EBER1 that was present in culture supernatants existed as a complex with EBER-binding cellular proteins. Flag-tagged L22, La, and PKR were transfected into Mutu+ cells, and their interaction with EBER1 in culture supernatants was examined by coimmunoprecipitation assays. Although flag-tagged L22, La, and PKR were expressed equally in transfected cells, only La could be strongly immunoprecipitated from the culture supernatant (Fig. 3 A). RT-PCR indicated that EBER1 preferentially coimmunoprecipitated with La (Fig. 3 B). The presence of La in culture supernatants suggested that La was actively secreted from living cells rather than passively released from dead cells. These results indicate that EBER1 was released from EBV-infected cells as a complex with La. To further assess whether EBER can activate TLR3 in complexes with La, we used immunoprecipitates

Published August 31, 2009

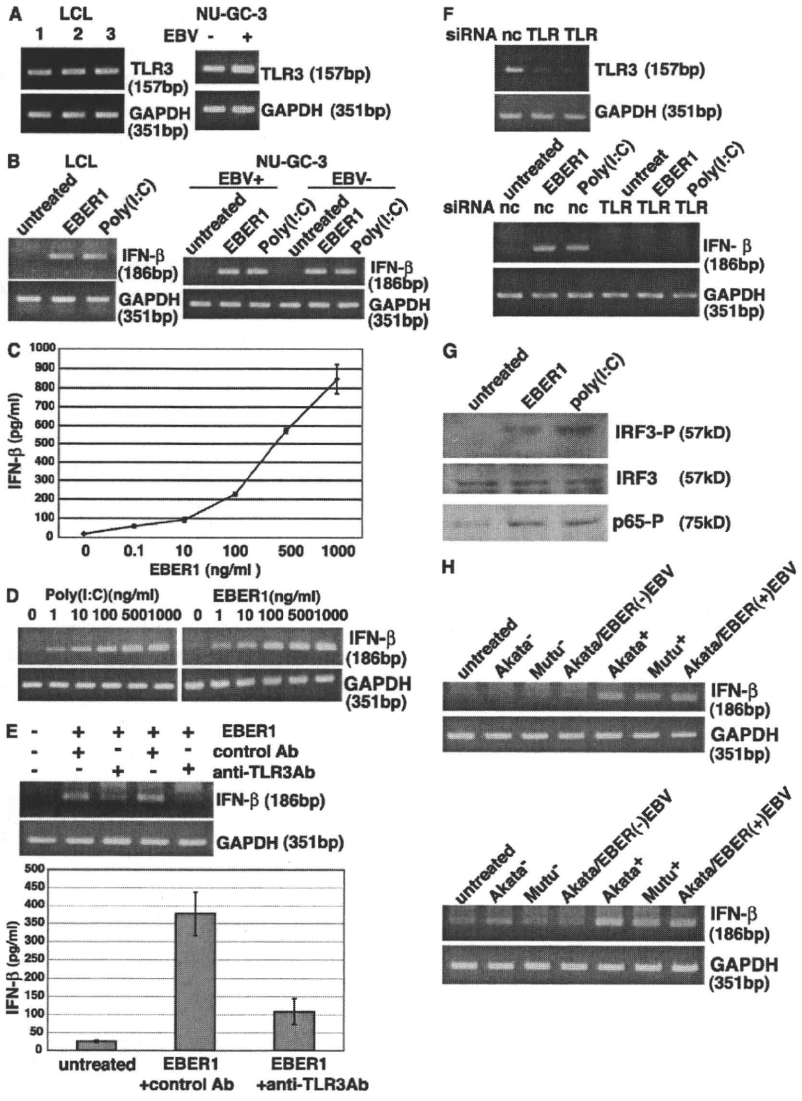

Figure 2. EBER1 activates signaling through TLR3. (A) Detection of TLR3 in three LCL clones and EBV-infected and uninfected NU-GC-3 cells. Total RNA (0.1 μg) was subjected to 30 cycles of RT-PCR to detect TLR3. RT-PCR for GAPDH was used as an internal control. Three or more independent experiments were performed for each assay. (B) Effect of in vitro–synthesized EBER1 on the expression of IFN-β. LCLs and EBV-positive and –negative NU-GC-3 cells were treated with 0.5 μg/ml in vitro–synthesized EBER1 or poly(I:C) and were cultured for 14 h. Total RNA (0.1 μg) was subjected to 30 cycles of RT-PCR to detect IFN-β. RT-PCR for GAPDH was used as an internal control. Three or more independent experiments were performed. (C) Dose response of the effect of in vitro–synthesized EBER1 on the expression of IFN-β. LCLs (4×10^5 cells/ml) were treated with 0.1–1,000 ng/ml EBER1 and cultured for 14 h. IFN-β in culture supernatants was quantified by ELISA. Error bars indicate the S.D. of duplicate wells. The data presented are representative of three independent experiments. (D) Efficiency of EBER1 and poly(I:C) to induce IFN-β expression in LCLs. LCLs (4×10^5 cells/ml) were treated with 1–1,000 ng/ml EBER1 and cultured for 14 h. IFN-β induction was analyzed by RT-PCR. Three or more independent experiments were performed for each assay. (E) Effect of an anti-TLR3 antibody on EBER1-induced IFN-β production. LCLs were preincubated with the anti-TLR3 antibody for 30 min at 37°C, before being treated with 0.5 μg/ml of EBER1 and incubated for 14 h. The culture was analyzed for IFN-β induction by RT-PCR (upper panel) and ELISA (lower panel). Error bars indicate the SD of duplicate wells. The data presented are representative of three independent experiments. (F) Effect of TLR3 knockdown on EBER1-induced IFN-β production. Negative control siRNA (nc) or TLR3-siRNA (TLR) were transfected into EBER-knockout EBV-infected AGS cells. After 48 h, cells were treated with EBER1 or poly(I:C) and IFN-β induction was analyzed by RT-PCR (bottom). Efficiency of TLR3 silencing was analyzed by RT-PCR (top). Three or more independent experiments were performed for each assay. (E) Effect of EBER1 on the downstream signals of TLR3, IRF3, and NF-κB. LCLs were treated with 2.5 μg/ml in vitro–synthesized EBER1 or poly(I:C) and cultured for 3 h before the phosphorylation of IRF3, and NF-κB was examined by immunoblotting using antibodies against phosphorylated IRF3, total IRF3, and phosphorylated p65. The data presented are representative of three independent experiments. (F) Effect of culture supernatants from EBER-positive cells on the expression of IFN-β. The study includes EBV-positive and –negative Mutu cells, EBV-positive and –negative Akata cells, and EBV-negative Akata cells that were stably infected with EBER-positive EBV or EBER-knockout EBV. The cells (2×10^5 cells/ml) were cultured for 4 d and then the culture supernatants were harvested. LCLs (4×10^5) were treated with 1 ml culture supernatants (top) or RNA extracted from 1 ml culture supernatants in 1 ml culture medium (bottom) for 14 h. RNA (0.1 μg) was subjected to 30 cycles of RT-PCR to detect IFN-β. Three or more independent experiments were performed for each assay.

Published August 31, 2009

from culture supernatants of EBV-positive or EBER-knockout EBV-infected cells for stimulation. EBV-positive and EBER-knockout EBV-infected AGS cells were transfected with Flag-La, and immunoprecipitates from culture supernatants were added into a culture medium of EBER-knockout EBV-infected AGS cells. As shown in Fig. 3 C, IFN-β was clearly induced by treatment with immunoprecipitates from culture supernatants of EBV-positive cells, whereas the IFN induction was reduced by TLR3 knockdown. In contrast, no IFN induction was observed in the cells treated with immunoprecipitates from culture supernatants of EBER-knockout EBV-infected cells. These results suggest that EBER1 can induce TLR3 signaling in complexes with La.

EBER1 exists in sera from patients with active EBV infections and induces the production of type I IFN and inflammatory cytokines

Subsequently, we examined the presence of EBER1 in the sera of patients with acute EBV infections, such as IM, CAEBV, and EBV-HLH. We also investigated the role of EBER on the activation of TLR3. Results from RT-PCR assays revealed that EBER1 was detected in patient sera and also in the sera from healthy individuals (Fig. 4 A); however, the level of EBER1 was much higher in patient sera than that obtained from healthy individuals. Our real-time PCR assays indicated that the sera contained 0.17 to 0.24 ng/ml of EBER1 (Fig. 4 B), which was sufficient to induce signaling from TLR3 (Fig. 2 C). Because we had demonstrated that sera nonspecifically induced IFN and cytokines in LCLs, we stimulated LCLs with RNA that had been purified from that sera. As shown in Fig. 4 C, RNAs from the patient sera, which contained a higher amount of EBER1, induced the release of IFN-β when added to the culture medium of LCLs. The quantification of IFN-β by ELISA indicated that all of the patient sera that we examined induced more IFN-β (200–800 pg/ml) than that induced by the sera from healthy individuals. To confirm that IFN-β induction by patient sera was mediated thorough TLR3, LCLs were pretreated with an anti-TLR3 antibody and treated with RNA from a patient serum with IM. The results demonstrate that there was a marked reduction in the RNA-induced release of IFN-β (Fig. 4 D), indicating that the RNA from serum induced the expression of IFN through TLR3. We also examined whether RNAs from the patient sera could induce type I IFN and proinflammatory cytokines such as IFN-γ and TNF in PBMCs. As shown in Fig. 4 E, RNAs purified from CAEBV, which contained a high level of EBER1, induced the expression of IFN-β, IFN-γ, and TNF.

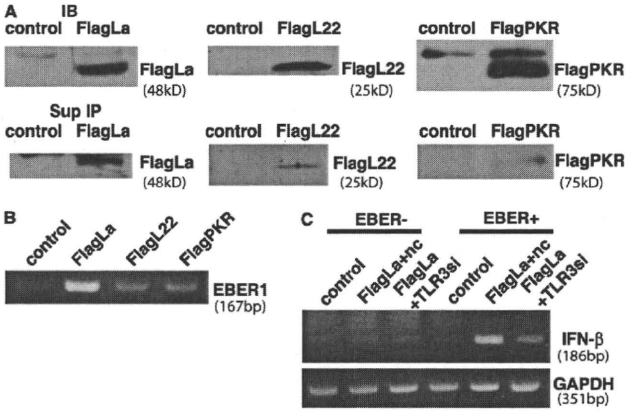

Figure 3. EBER is detected as a complex with La in the culture supernatants and the complex is stimulatory for TLR3. (A) Detection of La, L22, and PKR in culture supernatants. Mutu+ cells (1×10^6) were transfected with Flag-tagged La, L22, or PKR plasmid and cultured for 48 h. Flag-tagged La, L22, and PKR were detected by immunoblotting of the cell lysates (top) and immunoprecipitation of culture supernatants (bottom) using an anti-Flag antibody. Three or more independent experiments were performed for each assay. (B) Detection of EBER1 in the immunoprecipitates. RNA was extracted from the immunoprecipitates and subjected to 30 cycles of RT-PCR to detect EBER1. Three independent experiments were performed. (C) Effect of immunoprecipitates from culture supernatants on IFN-β induction. EBER-positive (EBER+) or EBER-knockout (EBER−) EBV-infected AGS cells were transfected with control (control) or Flag-tagged La plasmid (Flag La) and cultured for 48 h, followed by immunoprecipitation of culture supernatants using anti-Flag antibody. Both EBER− and EBER+ immunoprecipitates were added into the media of EBER-knockout EBV-infected AGS cells transfected with negative control siRNA (Flag La+nc) or TLR3 siRNA (Flag La+TLR3si), and IFN-β induction was analyzed by RT-PCR. The data presented are representative of three independent experiments.

EBER1 induces mature surface phenotype and antigen-presenting capacity of DCs

Finally, we investigated the effect of EBER1 on DC function to clarify whether EBER1-mediated signaling is sufficient for induction of immune responses. We treated immature DCs with EBER1 or poly(I:C) for 24 h and analyzed the surface markers of matured DC by flow cytometry. Treatment with EBER1, as well as poly(I:C), resulted in an increase of CD83 and CD86 levels, indicating that EBER1 induces maturation of DCs (Fig. 5 A). Because CD86 up-regulation by EBER1 was clearly reduced by TLR3 siRNA, EBER1-mediated DC maturation is dependent on TLR3 (Fig. 5 B). We next investigated cytokine production by DCs in response to EBER1. As shown in Fig. 5 C, IFN-β and IL-12 production by DCs was induced by EBER1, indicating EBER1-mediated activation of DCs. Furthermore, sera from patients containing a high level of EBER1 induced IL-12 production by DCs in a TLR3-dependent manner, whereas sera containing a low level of EBER1 or EBV-negative sera could not, suggesting that EBER1 in sera is stimulatory for DCs through TLR3 signaling (Fig. 5 D). To assess whether DCs with maturation induced via EBER1 have the capacity of antigen presentation, DCs treated with EBER1 or poly(I:C) were used for allo MLR assay. The stimulatory properties of EBER1- or poly (I:C)-treated DCs were compared with those of untreated immature DCs. As shown in Fig. 5 E, EBER1- or poly(I:C)-treated DCs induced comparable allo mixed lymphocyte reactions that were most markedly seen with 10,000 DCs/wells, in a 1:10 stimulator/responder ratios. Therefore,

Published August 31, 2009

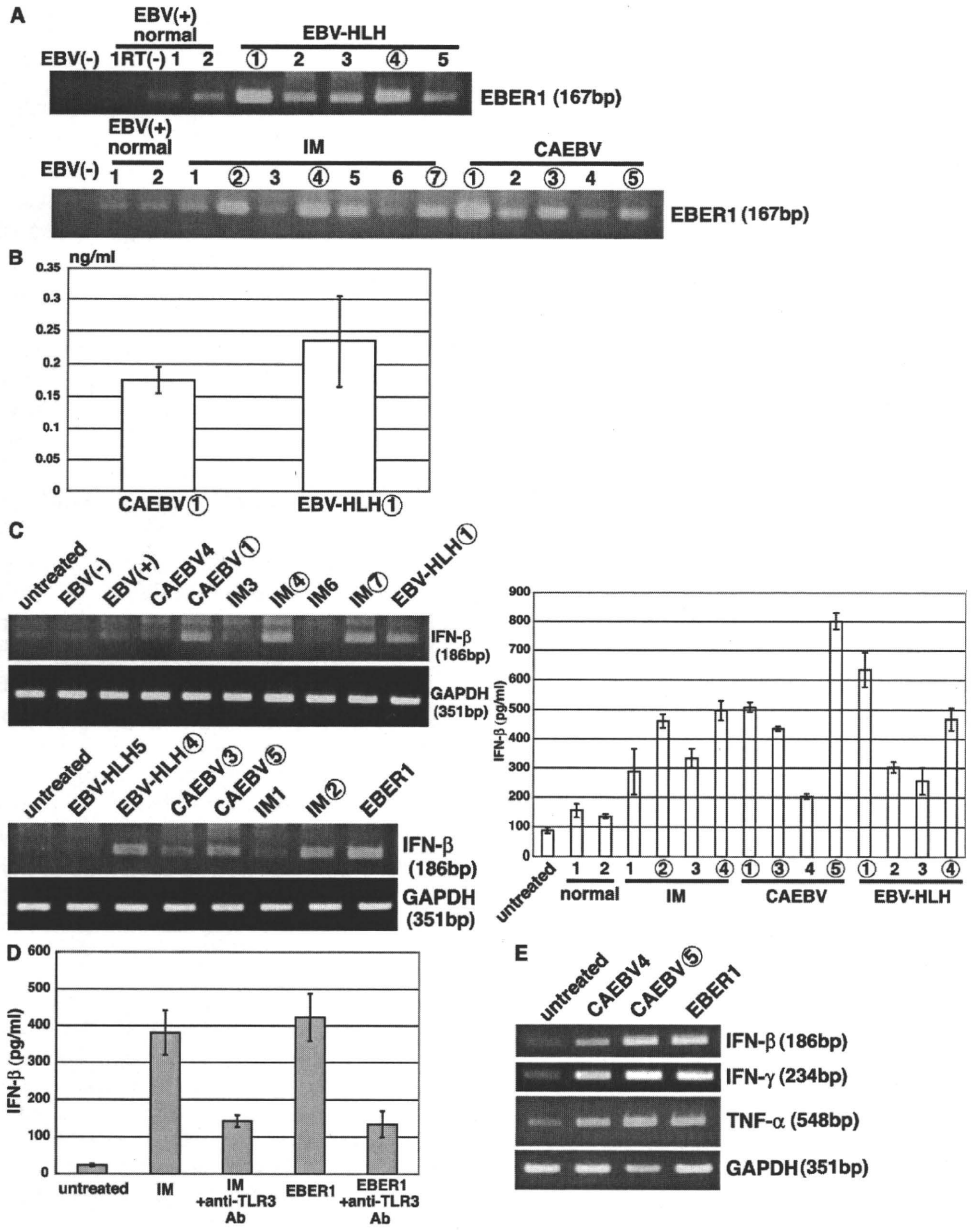

Figure 4. EBER1 exists in sera from patients with active EBV infections and induces the production of type I IFN and inflammatory cytokines. (A) Detection of EBER1 by RT-PCR in patient sera. RNA was extracted from 100 µl sera or plasma from patients with IM, CAEBV, and EBV-HLH, and from EBV-positive and –negative healthy donors. EBER1 was detected by 35 cycles of RT-PCR. Sample numbers in A–C correspond to each other; samples that are followed by a number in an open circle contain higher amounts of EBER1 than those with a number alone. Three or more independent experiments were performed. (B) Quantification of EBER1 in patient sera. RNA was extracted from the sera and subjected to real-time RT-PCR to detect EBER1. Error bars indicate the SD of duplicate wells. The data presented are representative of three independent experiments. (C) Induction of IFN-β production by RNA extracted from patient sera. LCLs (4×10^5) were treated with RNA that had been extracted from 100 µl sera in 1 ml culture medium, incubated for 14 h, and subjected to 30 cycles of RT-PCR to detect IFN-β (left) or ELISA of the culture supernatants for detection of IFN-β (right). The data of ELISA are shown as the means ± SD of duplicate determination and representative results of three independent experiments are shown. (D) Effect of an anti-TLR3 antibody on serum-induced IFN-β production. LCLs (4×10^5) were preincubated with the anti-TLR3 antibody for 30 min at 37°C, before being treated with RNA extracted from 100 µl of serum from a patient with IM or 1.0 µg in vitro–synthesized EBER1 as a positive control in 1 ml culture medium, and cultured for 14 h. Production of IFN-β was determined by ELISA of the culture supernatants. Error bars indicate the S.D. of duplicate wells. The data presented are representative of three independent experiments. (E) Effect of the RNA from patients sera on the induction of IFN-β and proinflammatory cytokines. Human PBMCs (1×10^6) were treated with RNA extracted from 100 µl patients sera or 0.5 µg in vitro–synthesized EBER1 in 1 ml culture medium and cultured for 14 h. The induction of IFN-β and proinflammatory cytokines was determined by 30 cycles of RT-PCR. Three independent experiments were performed.

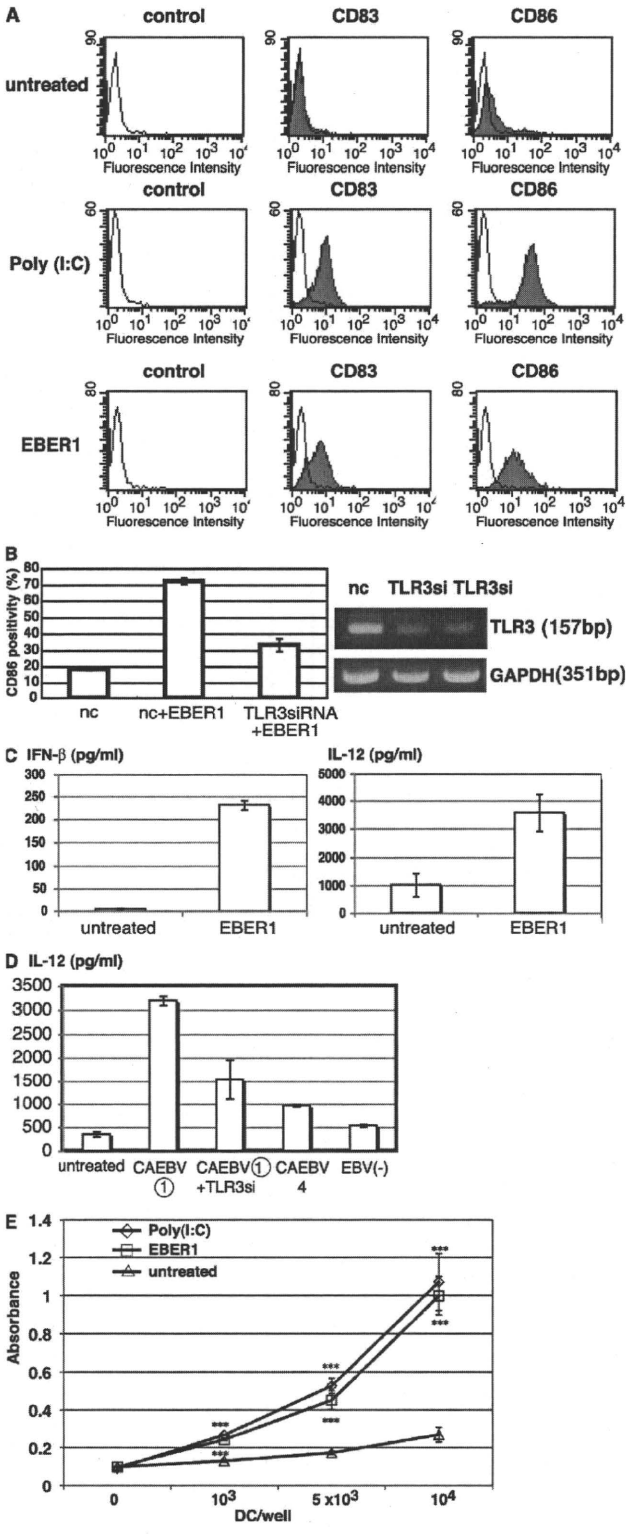

Figure 5. EBER1 induces maturation of DC and subsequent antigen presentation. (A) Effect of EBER1 on phenotype of DCs. DCs were prepared from PBMCs and untreated or treated with either poly(I:C) (10 μg/ml) or EBER1 (10 μg/ml). Surface markers of matured DCs, CD83, and CD86 were measured by flow cytometry. As negative control, cells were stained with mouse IgG. The data are representative of three independent experiments. (B) Effect of TLR3 knockdown on EBER1-mediated DC maturation. DCs were transfected with TLR3 siRNA or control siRNA (nc) and were stimulated with EBER1. CD86 positivity (%) was analyzed by flow cytometry (left). Efficiency of TLR3 silencing was analyzed by RT-PCR (right). Data are shown as the means ± SD of duplicate determination and representative results of three independent experiments are shown. (C) EBER1-induced cytokine production by DCs. DCs were treated with EBER1, and IFN-β or IL-12p40 production were measured by ELISA. Error bars indicate the SD of duplicate wells, and the data presented are representative of three independent experiments. (D) Effect of sera from patients on TLR3-mediated IL-12 production by DCs. DCs were transfected with negative control siRNA or TLR3 siRNA (TLR3si) for 48 h, and then stimulated with sera from patients with CAEBV containing high amounts of EBER1 (CAEBV (1)) and IL-12 production was measured by ELISA. Sera form patients with CAEBV containing low amounts of EBER1 (CAEBV4) or EBV-negative (EBV(−)) healthy donor were also used for stimulation. Data are shown as the means ± SD of duplicate determination and representative results of three independent experiments are shown. (E) Allogenic MLR. DCs treated with either poly(I:C) or EBER1 were used as stimulator cells. Untreated immature DC were also used as stimulator cells. Allogenic PBMCs (1×10^5) were used as responder cells in triplicate cultures. Proliferation of alloreactive T cells was determined by cell proliferation assay. Data are shown as the means ± SD of triplicate determination and representative results of three independent experiments are shown. Statistical significance differences between groups were evaluated by Student's *t* test. ***, $P < 0.001$.

EBER1-treated DCs were potent inducers of primary allo T cell responses.

In this study, we have demonstrated that EBER1 is released from EBV-infected cells and activates signaling from the TLR3. We have also demonstrated that sera from patients with active EBV infections such as IM, CAEBV, and EBV-HLH contained a large amount of EBER1, which was sufficient to activate TLR3 signaling, subsequently resulting in the induction of type I IFN and proinflammatory cytokines. Furthermore, EBER1-treated DCs could induce primary immune response, suggesting that during active infection, EBER1-mediated TLR3 stimulation is responsible for immune activation by EBV. TLR3 is predominantly expressed on DCs (Doyle et al., 2003; Akira and Takeda, 2004); circulating EBER1 could induce the activation of DCs and subsequent T cell activation, leading to the systemic production of proinflammatory cytokines. EBER1-mediated immune response would be needed for host defense, therefore IM, which is characterized as a CTL response against polyclonal proliferation of EBV-infected B cells usually follows a self-limited course. In EBV-HLH, EBV-infected cells are mainly $CD8^+$ T cells, whereas $CD4^+$ T or NK cells are infected in CAEBV (Kasahara et al., 2001). Given that $CD8^+$ T cells and NK cells express TLR3 and are activated by TLR3 signals (Schmidt et al., 2004; Tabiasco et al., 2006), TLR3-expressing T cells and NK cells could be activated by EBER1 through TLR3 and produce proinflammatory cytokines. Our findings suggest that immunopathologic diseases that are caused by active EBV infections could be attributed to TLR3-mediated cytokinemia

Published August 31, 2009

by EBER1, and that circulating EBER1 could be a potential target for therapeutic agents. Because it has been reported that plasmacytoid DCs are involved in anti-EBV immunity by the secretion of IFN and T cell activation through TLR9 pathways (Lim et al., 2007), TLR3 would collaborate with TLR9 during primary EBV infection.

Recent studies have demonstrated that activation of TLR3 by viral dsRNA contributes to viral pathogenesis. For example, TLR3-mediated inflammatory responses by viral dsRNA contribute to the development of lethal encephalitis by facilitating virus entry into the brain during West Nile virus infection (Wang et al., 2004). Rotavirus genomic dsRNA induces severe injury in the small intestine of mice in a TLR3-dependent manner (Zhou et al., 2007). These findings, along with ours, suggest that activation of TLR3 induces not only protective effects against viral infection but also effects that contribute to viral pathogenesis.

It was reported that EBER1 mostly binds to L22 (Toczyski and Steitz, 1993). Therefore, if EBER1 is released because of cell death, it would be released with Flag-L22 rather than other Flag-tagged proteins from the cell, in which those proteins are equally expressed. However, the majority of the EBER1 that was released from the cells existed in a complex with Flag-La, whereas other EBER-binding proteins, such as PKR and L22 were faintly detected. This led us to hypothesize that EBER1 is released from the cells by active secretion of La. Because La has been reported to be secreted as an exosome (Kapsogeorgou et al., 2005), EBER1 might also be secreted in this manner by binding to La. Alternatively, if La is more stable than L22 in extracellular state, EBER1 released by cell death could be strongly detected with La. Interestingly, we also demonstrated that EBER1 stimulates TLR3 in complexes with La protein. Further study is needed to clarify how the EBER1–protein complex is recognized by TLR3 and the mechanism of EBER1 release.

In contrast to EBER1, EBER2 was faintly detected in the culture supernatants of EBV-infected cells or in sera from patients with active EBV infections. EBER2 has a shorter half-life than EBER1, which may account for the preferential detection of EBER1 in our experiments (Clarke et al., 1992).

MATERIALS AND METHODS

Cell culture and reagents. LCLs, the EBV-positive Burkitt's lymphoma cell lines Akata+ (Takada, 1984) and Mutu+ (Gregory et al., 1990), and the EBV-negative cell lines Akata− (Shimizu et al., 1994) and Mutu− (Nanbo et al., 2002) were cultured in RPMI 1640 media (Sigma-Aldrich) supplemented with 10% FBS (Invitrogen) and antibiotics. Akata− cells that had been reinfected with recombinant EBER-positive EBV (Akata/EBER$^+$EBV; Shimizu et al., 1996) or EBER-knockout EBV (Akata/EBER$^-$EBV; Yajima et al., 2005) were cultured in RPMI 1640 media containing 700 μg/ml G418 (Sigma-Aldrich). EBV-infected (EBV+) and neomycin-resistant gene transfected (EBV−) NU-GC-3 cells and EBER-positive EBV or EBER-knockout EBV-infected AGS cells were cultured in Dulbecco's modified Eagle's medium (Sigma-Aldrich) supplemented with 10% FBS, antibiotics, and 500 μg/ml G418. The anti-Flag antibody and mouse IgG1 were purchased from Sigma-Aldrich. The anti-TLR3 antibody was obtained from eBioscience, and the anti-phospho IRF3 antibody, anti-IRF3 antibody, and anti-phospho p65 antibody were obtained from Cell Signaling Technology. poly(I:C) and polymyxin B were purchased from EMD. Anti-CD83 antibody and anti-CD86 antibody were obtained from Beckman Coulter and Ancell Co., respectively. Human recombinant GM-CSF and IL-4 were purchased from PeproTech.

RNA extraction and RT-PCR. Total RNA was extracted using Trizol reagent (Invitrogen) and was treated with DNaseI (Invitrogen). To analyze the release of EBER, RNA was extracted from 1 ml culture media or 100 μl serum and plasma. Reverse transcription was performed using SuperScript II reverse transcription (Invitrogen) and oligo-dT primer (Promega) or sequence-specific primers for EBER1 and EBER2. The sequence of the primers used for PCR was as follows. EBER1 (5′-AGGACCTACGCTGCCCTAGA-3′, 5′-AAAACATGCGGACCAGC-3′), EBER2 (5′-AGGGACAGCCGTTGCCCTAGTGGTTTCGGA-3′, 5′-AAAACAGCGGACAAGCCGAATACC-3′), TLR3 (5′-TCACTTGCTCATTCTCCCTT-3′, 5′-GACCTCTCCATTCCTGGC-3′), IFN−β (5′-GATTCATCGAGCACTGGCTGG-3′, 5′-CTTCAGGTAATGCAGAATCC-3′), IFN-γ (5′-CAGGTCATTCAGATGTAGCG-3′, 5′-GCTTTTCGAAGTCATCTCG-3′), TNF (5′-CTTCTGCCTGCTGCACTTTGGA-3′, 5′-TCCCAAAGTAGACCTGCCCAGA-3′), and GAPDH (5′-GCCTCCTGCACCACCAACTG-3′, 5′-CGACGCCTGCTTCACCACCTTCT-3′).

Quantification of EBER1. EBER1 was prepared by in vitro transcription as previously described (Samanta et al., 2006). Serial dilutions of EBER1 (0.1 ng/ml to 1.0 μg/ml) were made in culture media and total RNA was extracted and used for real-time PCR using the LightCycler system (Roche). These results were used as a standard for measuring the amount of EBER1 in culture supernatant.

Analysis of TLR3 activation. In vitro–synthesized EBER1 or poly(I:C) and RNAs that had been prepared from culture supernatants or human sera were mixed with Lipofectamine 2000 (Invitrogen) for 15 min in Opti-MEM (Invitrogen) before being used to stimulate the cells. The reagents were incubated in the tissue culture medium for 1 h before being removed by washing. To neutralize TLR3, cells were pretreated with an anti-TLR3 antibody (40 μg/ml) for 30 min at 37°C. The antibody was then removed before the TLR3 stimulation.

Measurement of cytokine production. Cell culture supernatants were collected and analyzed for IFN-β and IL-12 p40 production using a human IFN-β ELISA kit (PBL Biomedical Laboratories) or OptEIA human IL-12 (p40) ELISA kit (BD) according to the manufacturer's protocol.

Immunoblotting. Cells were lysed with 1% NP-40 lysis buffer and the cell lysates were subjected to SDS-PAGE and subsequent electrotransfer onto nitrocellulose membranes. The membranes were blocked with 5% bovine serum albumin (Sigma-Aldrich) or nonfat milk in TBS containing 0.05% Tween 20, and were subsequently treated with the primary antibodies for phospho-IRF3, IRF-3, phospho-p65, and the Flag tag.

Analysis of EBER-protein interactions by coimmunoprecipitation. Mutu cells (2×10^6) were transfected with Flag-La, Flag-L22, and Flag-PKR expression plasmids by electroporation. After 48 h, 1 ml culture supernatant was harvested and incubated with 3.5 μg anti-Flag mouse monoclonal antibody for 14 h at 4°C. After the addition of 50 μl of protein G–Sepharose (GE Healthcare), mixtures were incubated at 4°C for 3 h. Sepharose beads were pelleted and washed twice with lysis buffer (50 mM Tris-HCl, pH 7.4, 150 mM NaCl, 1% Nonidet P-40, 0.5% deoxycholate, and 20% protease/inhibitor) and three times with wash buffer (50 mM Tris-HCl, pH 7.4, 200 mM NaCl, 0.1% Nonidet P-40, 0.05% deoxycholate, 10% protease/inhibitor mix, 100 units/ml RNasin, 0.4% vanadyl ribonucleoside complex, and 1 mM dithiothreitol) by end-over-end rotation for 10 min. Pellets were dissolved in SDS loading buffer and subjected to immunoblotting. For RNA extraction, pellets were dissolved in 100 μl of lysis buffer and digested with 30 μg of proteinase K for 30 min at 50°C with the addition of 0.1% SDS,

before being dissolved in Trizol reagent. Extracted RNA was analyzed by RT-PCR for the expression of EBER1.

Flow cytometry. Cells were washed with FACS buffer (PBS containing 0.1% BSA, 0.1% NaN_3) and stained with anti-CD83 antibody (1 μg), anti-CD86 antibody (0.5 μg), or mouse IgG1 (1 μg) together with human IgG (10 μg) for 30 min at 4°C. After washing twice with FACS buffer, cells were incubated with FITC-labeled secondary antibody (American Qualex) for 30 min at 4°C, and then analyzed on a FACSCalibur (BD).

Preparation and stimulation of DCs. The institutional committee at Hokkaido University approved the use of human blood samples for this study. $CD14^+$ monocytes were isolated from human PBMC using a MACS system (Miltenyi Biotec). Immature DCs were generated from monocytes by culture for 6 d in RPMI 1640 medium supplemented with 10% heat-inactivated FCS (SAFC Biosciences) in the presence of 500 IU/ml recombinant human GM-CSF and 100 IU/ml recombinant human IL-4. Immature DCs (10^6 cells/ml) were treated with poly(I:C) (10 μg/ ml) or synthesized EBER1 (10 μg/ml) for 24 h. Both reagents were treated with polymyxin B (5 μg/ml) at 37°C for 1 h before stimulation.

TLR3 knockdown experiment. TLR3 stealth RNAi (Invitrogen) or stealth RNAi negative control (Invitrogen) was transfected using Lipofectamine RNAiMAX (Invitrogen) according to the manufacturer's protocol. Successful transfection was confirmed using the BLOCK-iT Alexa Fluor Red Fluorescent Oligo (Invitrogen). Monocytes were cultured for 4 d before being transfected (10^6 cells/well, 24 well plate) on day 4 and again on day 5 with 70 nM siRNA. On day 6 (48 h after the first transfection), cells were used for stimulation. AGS cells (10^5 cells/well, 24-well plate) were transfected with 10 nM siRNAs and used for stimulation after 48 h.

Mixed lymphocyte reaction (MLR) assay. After 24 h stimulation with poly(I:C) or EBER1, DCs were treated with 50 μg/ml mitomycin C (MMC). Allo-PBMC were isolated by Histopaque density gradient separation of blood collected from healthy donors. Serial dilutions (10^4 to 10^3 cells/well) of MMC-treated DCs were cultured in triplicate with 10^5 PBMCs in 96-well round-bottom plates for 3 d, and PBMC proliferation was measured using CellTiter 96 nonradioactive cell proliferation assay kit (Promega).

We thank Y. Ando for technical assistance.

This work was supported by grants-in-aid from the Ministry of Education, Science, Sports, Culture and Technology, Japan (D. Iwakiri and K. Takada) and by the Takeda Science Foundation and the Akiyama Foundation (D. Iwakiri).

The authors have no conflicting financial interests.

Submitted: 7 August 2008
Accepted: 10 August 2009

REFERENCES

Akira, S., and K. Takeda. 2004. Toll-like receptor signalling. *Nat. Rev. Immunol.* 4:499–511. doi:10.1038/nri1391

Akiyama, S., H. Amo, T. Watanabe, M. Matsuyama, J. Sakamoto, M. Imaizumi, H. Ichihashi, T. Kondo, and H. Takagi. 1988. Characteristics of three human gastric cancer cell lines, NU-GC-2, NU-GC-3 and NU-GC-4. *Jpn. J. Surg.* 18:438–446. doi:10.1007/BF02471470

Clarke, P.A., M. Schwemmle, J. Schickinger, K. Hilse, and M.J. Clemens. 1991. Binding of Epstein-Barr virus small RNA EBER-1 to the double-stranded RNA-activated protein kinase DAI. *Nucleic Acids Res.* 19:243–248. doi:10.1093/nar/19.2.243

Clarke, P.A., N.A. Sharp, and M.J. Clemens. 1992. Expression of genes for the Epstein-Barr virus small RNAs EBER-1 and EBER-2 in Daudi Burkitt's lymphoma cells: effects of interferon treatment. *J. Gen. Virol.* 73:3169–3175. doi:10.1099/0022-1317-73-12-3169

Doyle, S.E., R. O'Connell, S.A. Vaidya, E.K. Chow, K. Yee, and G. Cheng. 2003. Toll-like receptor 3 mediates a more potent antiviral response than Toll-like receptor 4. *J. Immunol.* 170:3565–3571.

Gregory, C.D., M. Rowe, and A.B. Rickinson. 1990. Different Epstein-Barr virus-B cell interactions in phenotypically distinct clones of a Burkitt's lymphoma cell line. *J. Gen. Virol.* 71:1481–1495. doi:10.1099/0022-1317-71-7-1481

Imai, S., J. Nishikawa, and K. Takada. 1998. Cell-to-cell contact as an efficient mode of Epstein-Barr virus infection of diverse human epithelial cells. *J. Virol.* 72:4371–4378.

Kapsogeorgou, E.K., R.F. Abu-Helu, H.M. Moutsopoulos, and M.N. Manoussakis. 2005. Salivary gland epithelial cell exosomes: a source of autoantigenic ribonucleoproteins. *Arthritis Rheum.* 52:1517–1521. doi:10.1002/art.21005

Kasahara, Y., A. Yachie, K. Takei, C. Kanegane, K. Okada, K. Ohta, H. Seki, N. Igarashi, K. Maruhashi, K. Katayama, et al. 2001. Differential cellular targets of Epstein-Barr virus (EBV) infection between acute EBV-associated hemophagocytic lymphohistiocytosis and chronic active EBV infection. *Blood.* 98:1882–1888. doi:10.1182/blood.V98.6.1882

Kikuta, H., Y. Sakiyama, S. Matsumoto, T. Oh-Ishi, T. Nakano, T. Nagashima, T. Oka, T. Hironaka, and K. Hirai. 1993. Fatal Epstein-Barr virus-associated hemophagocytic syndrome. *Blood.* 82:3259–3264.

Lerner, M.R., N.C. Andrews, G. Miller, and J.A. Steitz. 1981. Two small RNAs encoded by Epstein-Barr virus and complexed with protein are precipitated by antibodies from patients with systemic lupus erythematosus. *Proc. Natl. Acad. Sci. USA.* 78:805–809. doi:10.1073/pnas.78.2.805

Lim, W.H., S. Kireta, G.R. Russ, and P.T. Coates. 2007. Human plasmacytoid dendritic cells regulate immune responses to Epstein-Barr virus (EBV) infection and delay EBV-related mortality in humanized NOD-SCID mice. *Blood.* 109:1043–1050. doi:10.1182/blood-2005-12-024802

Matsumoto, M., S. Kikkawa, M. Kohase, K. Miyake, and T. Seya. 2002. Establishment of a monoclonal antibody against human Toll-like receptor 3 that blocks double-stranded RNA-mediated signaling. *Biochem. Biophys. Res. Commun.* 293:1364–1369. doi:10.1016/S0006-291X(02)00380-7

Nanbo, A., K. Inoue, K. Adachi-Takasawa, and K. Takada. 2002. Epstein-Barr virus RNA confers resistance to interferon-α-induced apoptosis in Burkitt's lymphoma. *EMBO J.* 21:954–965. doi:10.1093/emboj/21.5.954

Rickinson, A.B., and E. Kieff. 2001. Epstein-Barr virus. *In* Fields Virology. Fourth edition. B.N. Fields, D.M. Knipe, and P.M. Howley, editors. Lippincott Williams & Wilkins, Philadelphia. 2575–2627.

Rosa, M.D., E. Gottlieb, M.R. Lerner, and J.A. Steitz. 1981. Striking similarities are exhibited by two small Epstein-Barr virus-encoded ribonucleic acids and the adenovirus-associated ribonucleic acids VAI and VAII. *Mol. Cell. Biol.* 1:785–796.

Rymo, L. 1979. Identification of transcribed regions of Epstein-Barr virus DNA in Burkitt lymphoma-derived cells. *J. Virol.* 32:8–18.

Samanta, M., D. Iwakiri, T. Kanda, T. Imaizumi, and K. Takada. 2006. EB virus-encoded RNAs are recognized by RIG-I and activate signaling to induce type I IFN. *EMBO J.* 25:4207–4214. doi:10.1038/sj.emboj.7601314

Schmidt, K.N., B. Leung, M. Kwong, K.A. Zarember, S. Satyal, T.A. Navas, F. Wang, and P.J. Godowski. 2004. APC-independent activation of NK cells by the Toll-like receptor 3 agonist double-stranded RNA. *J. Immunol.* 172:138–143.

Shimizu, N., A. Tanabe-Tochikura, Y. Kuroiwa, and K. Takada. 1994. Isolation of Epstein-Barr virus (EBV)-negative cell clones from the EBV-positive Burkitt's lymphoma (BL) line Akata: malignant phenotypes of BL cells are dependent on EBV. *J. Virol.* 68:6069–6073.

Shimizu, N., H. Yoshiyama, and K. Takada. 1996. Clonal propagation of Epstein-Barr virus (EBV) recombinants in EBV-negative Akata cells. *J. Virol.* 70:7260–7263.

Tabiasco, J., E. Devêvre, N. Rufer, B. Salaun, J.C. Cerottini, D. Speiser, and P. Romero. 2006. Human effector CD8+ T lymphocytes express TLR3 as a functional coreceptor. *J. Immunol.* 177:8708–8713.

Takada, K. 1984. Cross-linking of cell surface immunoglobulins induces Epstein-Barr virus in Burkitt lymphoma lines. *Int. J. Cancer.* 33:27–32. doi:10.1002/ijc.2910330106

Toczyski, D.P., and J.A. Steitz. 1993. The cellular RNA-binding protein EAP recognizes a conserved stem-loop in the Epstein-Barr virus small RNA EBER 1. *Mol. Cell. Biol.* 13:703–710.

Published August 31, 2009

Toczyski, D.P., A.G. Matera, D.C. Ward, and J.A. Steitz. 1994. The Epstein-Barr virus (EBV) small RNA EBER1 binds and relocalizes ribosomal protein L22 in EBV-infected human B lymphocytes. *Proc. Natl. Acad. Sci. USA.* 91:3463–3467. doi:10.1073/pnas.91.8.3463

Wang, T., T. Town, L. Alexopoulou, J.F. Anderson, E. Fikrig, and R.A. Flavell. 2004. Toll-like receptor 3 mediates West Nile virus entry into the brain causing lethal encephalitis. *Nat. Med.* 10:1366–1373. doi:10.1038/nm1140

Yajima, M., T. Kanda, and K. Takada. 2005. Critical role of Epstein-Barr Virus (EBV)-encoded RNA in efficient EBV-induced B-lymphocyte growth transformation. *J. Virol.* 79:4298–4307. doi:10.1128/JVI.79.7.4298-4307.2005

Zhou, R., H. Wei, R. Sun, and Z. Tian. 2007. Recognition of double-stranded RNA by TLR3 induces severe small intestinal injury in mice. *J. Immunol.* 178:4548–4556.

Surg Today (2009) 39:194–200
DOI 10.1007/s00595-008-3826-3

SURGERY TODAY

Original Articles

Innate Immune Therapy with a Bacillus Calmette-Guérin Cell Wall Skeleton After Radical Surgery for Non-Small Cell Lung Cancer: A Case–Control Study

KEN KODAMA[1], MASAHIKO HIGASHIYAMA[1], KOJI TAKAMI[1], KAZUYUKI ODA[1], JIRO OKAMI[1], JUN MAEDA[1], TAKASHI AKAZAWA[2], MISAKO MATSUMOTO[3], TSUKASA SEYA[3], MARIKO WADA[4], and KUMAO TOYOSHIMA[5]

Departments of [1]Thoracic Surgery and [2]Immunology, Osaka Medical Center for Cancer and Cardiovascular Diseases, 1-3-3 Nakamichi, Higashinari-ku, Osaka 537-8511, Japan
[3]Department of Microbiology and Immunology, Hokkaido University Graduate School of Medicine, Sapporo, Japan
[4]Mino Health Center, Mino, Japan
[5]SNP Research Center, RIKEN Yokohama Institute, Yokohama, Japan

Abstract

Purpose. We investigated whether adjuvant immunotherapy with Bacillus Calmette-Guérin (BCG) cell wall skeleton (CWS) and surgical resection was better than resection, with or without other adjuvant therapy, for patients with non-small cell lung cancer (NSCLC).

Methods. The case group comprised 71 patients who underwent radical surgery for NSCLC, followed by BCG-CWS immunotherapy, with follow-up data available. The case–control study was designed with one control selected for each case-group patient. Each control was matched by pathological stage and year of birth (±5 years). BCG-CWS 200 μg was inoculated intracutaneously in the upper arm four times per week (sensitization phase); then at 4-week intervals (therapeutic phase).

Results. The case-group patients received 45 ± 22.6 (average ± SD) cycles of BCG-CWS inoculation. Overall 5-year and 10-year survival rates were 71% and 61% for the case-group patients, and 63% and 43% for the control-group patients. The survival rate of the case group was better than that of the control group (not significant; $P = 0.114$). The same trend was seen in the patients with stage III or N+ NSCLC (not significant; $P = 0.114$, $P = 0.168$). There were no life-threatening adverse events.

Conclusions. BCG-CWS immunotherapy seemed to improve survival after resection of NSCLC, especially locally advanced NSCLC. Moreover, this immunotherapy did not compromise quality of life during treatment.

Key words Bacillus Calmette-Guérin cell wall skeleton · Immunotherapy · Non-small cell lung cancer · Surgical resection · Case–control study

Introduction

The human immune system consists of innate and acquired arms. Recent advances in the field of tumor immunology have revealed two novel findings in these two systems: first, most solid tumors express tumor-associated antigens (TAAs) which are rooted in the aberrance of tumor-related genes;[1] and second, activation of the innate immune system before the acquired system is indispensable for full activation of lymphocyte effectors, or cell-mediated immunity.[2] Considering the former issue, immunotherapy for cancer has been designed with TAA peptides and many cytokines, and this augments lymphocyte-based therapies.[3] Rosenberg et al. challenged clinical trials of a peptide vaccine therapy in which a variety of TAAs were administered to melanoma patients. However, the overall rate of remission (including incomplete remission) was only 2.6%.[4] They used peptide vaccines without adjuvant conjugated, or only with aluminum (non-Toll-like receptor (TLR)-directed adjuvant). These results suggest that innate immunity must be stimulated before the induction of acquired effectors to raise antitumor therapeutic potential.

Microbial components that activate the host innate immune system have been designated as adjuvants. Adjuvants are often used for immunization with pure antigens (Ag) for effective induction of antibody (Ab) production, cytotoxic T cells (CTL), and natural killer (NK) cell activation.[5] Many adjuvants have been identified as ligands for microbial pattern-recognition recep-

Reprint requests to: K. Kodama
Received: January 20, 2008 / Accepted: May 22, 2008

tors such as TLRs.[6] Through sensing microbe patterns, dendritic cells mature to present extrinsic Ag and release lymphocytes from an anergic state.[2,6] The cell-mediated immune system is thereafter activated to target Ag-bearing cells. This concept was demonstrated only recently, and it is now apparent that TLR agonists were being used as popular adjuvants for therapeutic purposes without knowledge of their mechanistic function.

For more than 6 years, clinical trials of many TLR-directed adjuvants have been conducted, aiming at adjuvant-augmented immunotherapy.[6,7] Most of these trials are still in progress with fruitful or anticipated results. Our earlier studies suggested that Bacillus Calmette-Guérin cell wall skeleton (BCG-CWS) has the potential to activate human antigen-presenting dendritic cells and induce interleukin 6 (IL-6), IL-12, tumor necrosis factor alpha (TNF-α),[8] and possibly, CTL.[9] Interferon-gamma (IFN-γ) levels increase in response to BCG-CWS.[10] A sole BCG-CWS without peptides was used in these studies since cancer patients are usually exposed to their own TAAs.[10] Studies on mouse tumor implant models suggest that BCG-CWS induces cross-priming facilitating class I presentation of exogenous antigens.[9] An efficient CTL response against Ag-bearing cells appears evident. These immune responses are attributed to TLR2 and TLR4 in antigen-presenting dendritic cells.[8,11]

The current clinical study was designed to investigate these basic findings on BCG-CWS adjuvant. We anticipated that BCG-CWS alone has the ability to evoke an antitumor immune response because patients with cancer postoperatively still possess TAAs.[10,12] To find out if patients who undergo radical surgery followed by adjuvant BCG-CWS immunotherapy for NSCLC are more likely to have a favorable outcome, we conducted a case–control study.

Materials and Methods

Preparation of BCG-CWS and Its Inoculation Schedule

BCG-CWS, donated by Dr. Azuma,[13] was used as an immunotherapeutic agent in the form of an oil-in-water emulsion, using either mineral oil (Drakeol 6VR) or a metabolizable oil such as squalene or squalane. After sterilizing by heating for 30 min at 60°C, the oil-attached BCG-CWS suspension was inoculated intracutaneously at a final concentration of 1 mg/ml in the upper arm according to the schedule described by Hayashi et al.[12,14] In the sensitization phase, 200 μg was inoculated four times weekly, whereas in the therapeutic phase, the amount inoculated, at 4-week intervals, ranged between 10 and 200 μg, depending on the patient's biological responses, including IFN-γ induction, local skin reaction at the inoculation site, various physical conditions (fever or general malaise), and indicators of laboratory tests showing liver function or inflammatory reactions.

Interferon-γ Induction Test

To evaluate the effect of immunotherapy on BCG-CWS, an IFN-γ induction test was performed at the time of the fourth inoculation in the sensitization phase, and at the time of the first and sixth inoculations in the therapeutic phase. The level of IFN-γ in the peripheral blood was measured before inoculation and 18 h after inoculation. Interferon-γ levels were detected with an enzyme-linked immunosorbent assay at the laboratory of Otsuka Assay (Tokushima, Japan), with the lower limit of sensitivity for detecting human serum IFN-γ being 7.8 pg/ml.

Case–Control Study

In May 1994, the protocol of a pilot study on BCG-CWS immunotherapy for patients with various malignant neoplasms was approved by the Ethical Review Board of Osaka Medical Center for Cancer and Cardiovascular Diseases. At the time of informed consent, we explained to patients about the expected effectiveness and side effects based on previous reports on immunotherapy,[15] chemotherapy,[16] and our survival data of surgery alone. In the 1990s, with the exception of one article published in 1995 from the NSCLC Collaborative Group,[16] there was no clear evidence of the survival benefit of adjuvant chemotherapy for NSCLC.

Written informed consent was obtained from all patients who chose to be treated with immunotherapy, which was started 4–6 weeks after the operation. Among the patients who received BCG-CWS, we recruited 83 NSCLC patients. Between 1994 and 2000, these patients received immunotherapy with BCG-CWS alone as adjuvant therapy after radical surgery for NSCLC. Since the clinical records of 12 patients were unavailable because their operations had been performed at other hospitals, they were excluded from the final analysis. Thus, 71 patients with both clinical records and follow-up data were enrolled in this study as the case group. They did not receive any other adjuvant therapy until recurrence was confirmed.

The case–control study was designed with one control selected for each patient. The control was matched to the patient by pathological stage and year of birth (±5 years). The matched control was recruited from among patients who underwent radical surgery for NSCLC, regardless of adjuvant chemo- and/or radiotherapy, with the shortest interval between the operation from our medical history data file.

Adverse effects of immunotherapy were graded from 0 (none) to 5 (fatal) according to the Common Terminology Criteria for Adverse Events; version 3 (CTCAE) of the National Cancer Institute.

Statistical Analysis

Continuous variables were analyzed by the *t*-test, and categorical variables were evaluated using χ^2 analysis. Overall survival rates and survival rates at each stage were compared between the patients and controls. We performed survival analysis with StatView version 5 (Abacus Computer, Berkeley, CA, USA), and survival curves were calculated with the Kaplan–Meier method.[17] Differences in survival were evaluated with the log-rank test. A P value of less than 0.05 was considered significant.

Results

The case-group patients were inoculated with 45 ± 22.6 (average ± SD) cycles of BCG-CWS over a range of 6–94 cycles (Fig. 1). Table 1 compares the patient characteristics of the case group with the control group. There were no significant differences between the groups in matched criteria, pathological stage (P = 1.000), or histology (P = 0.913). The mean age of the case-group patients was slightly less than that of the control patients (P = 0.087). The male to female ratio of the case-group patients was slightly lower than that of the control patients (P = 0.217). The types of lung resection and the pathological T and N factors were similar in the two groups (P = 0.967, 0.986, and 0.980, respectively). Among 40 control patients with stage II or III disease, 5 had received adjuvant chemo- and/or radiation therapy. The median follow-up was longer than 5 years and was similar in the two groups.

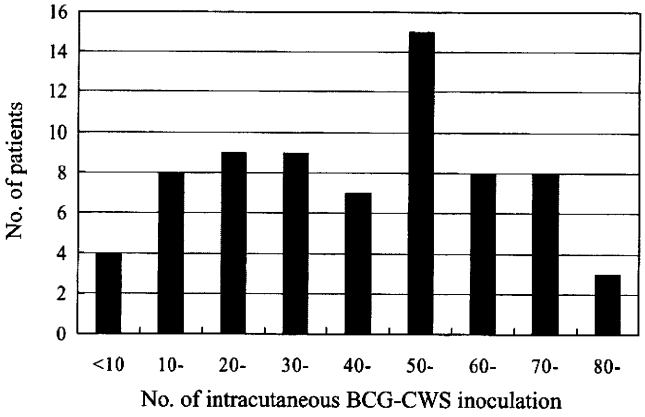

Fig. 1. Postoperative adjuvant immunotherapy with Bacillus Calmette-Guérin cell wall skeleton (*BCG-CWS*) for non-small cell lung cancer. Patient distribution according to the number of treatment courses

Table 1. Case–control study: patient backgrounds

Characteristic	Case patients	Control patients	*P* value
No. of patients	71	71	
Age, years (mean, range)	59 (37–78)	62 (38–78)	0.087
Sex			0.217
Male	43	50	
Female	28	21	
Surgery			0.967
Lesser resection	8	9	
Lobectomy	58	57	
Pneumonectomy	5	5	
Pathological T factor			0.986
T1	36	35	
T2	22	24	
T3	12	11	
T4	1	1	
Pathological N factor			0.980
N0	38	37	
N1	18	19	
N2	15	15	
Pathological stage			1.000
I	31	31	
II	21	21	
III	19	19	
Histology			0.913
Adenocarcinoma	51	49	
Squamous cell carcinoma	16	17	
Large cell carcinoma	4	5	
Median follow-up period (months)	68	66	

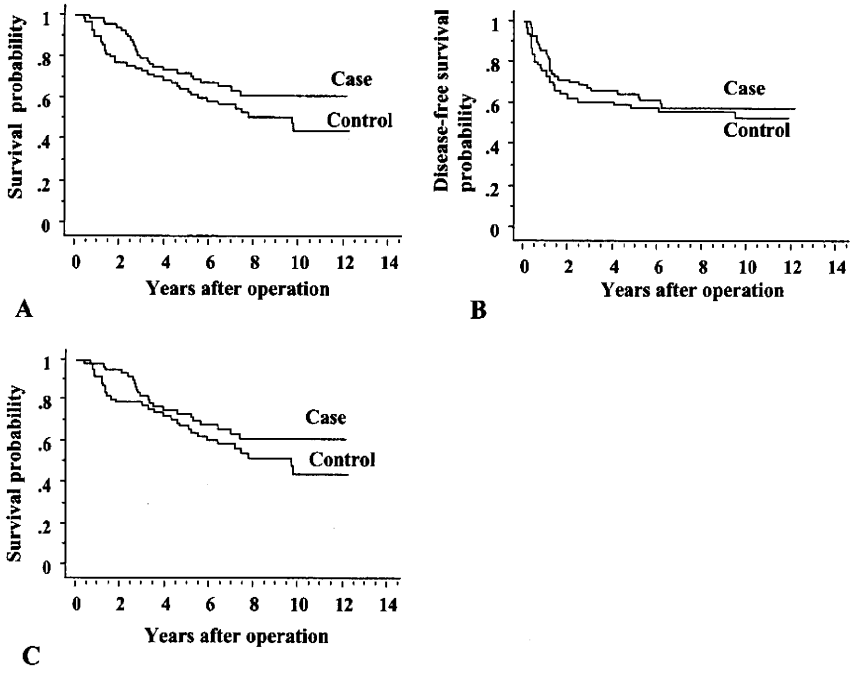

Fig. 2A–C. Kaplan–Meier overall survival estimates. **A** Survival curves. Case-group patients ($n = 71$) versus controls ($n = 71$). $P = 0.114$. **B** Disease-free survival curves. Case-group patients ($n = 71$) versus controls ($n = 71$). $P = 0.473$. **C** Survival curves of 62 gender-matched pairs. Case-group patients ($n = 62$) versus controls ($n = 62$). $P = 0.190$

When patients who had undergone radical surgery for NSCLC hoped to receive adjuvant immunotherapy in spite of a weak IFN-γ induction, the immunotherapy was continued if they had a local skin reaction at the injection site of BCG-CWS, such as an area of erythema greater than 20 mm in diameter, or an induration with an ulcer.[18] As a result, none of the patients given immunotherapy as postoperative adjuvant therapy stopped receiving it. The 5-year and 10-year survival rates were 74% and 62%, respectively, for 20 case-group patients given IFN-γ induction of 35 pg/ml or more, and 70% and 60%, respectively, for 39 given IFN-γ induction of less than 35 pg/ml ($P = 0.700$). The IFN-γ assay was not done for 12 patients.

The overall 5-year and 10-year survival rates were 71% and 61%, respectively, for the case-group patients, and 63% and 43%, respectively, for the control patients group (Fig. 2A). Although the difference was not significant, the survival rate of the case-group patients was better than that of the controls over the observation period ($P = 0.114$). The same trend was observed in disease-free survival between these two groups (Fig. 2B).

To exclude the influence of gender heterogeneity (Table 1) on survival, we selected 62 gender-matched pairs and compared their survival curves. The 5-year and 10-year survival rates were 73% and 61%, respectively, for the 62 case-group patients, and 67% and 44%, respectively, for the 62 control patients ($P = 0.190$; Fig. 2C).

According to the pathological stages, there were no significant differences in survival between the case and control group patients with stage I or II disease (Fig. 3A and 3B). The survival rate of the case-group patients with stage III disease was better than that of the control group patients with stage III disease, although the difference did not reach significance ($P = 0.114$; Fig. 3C). Ten multi-station N2 patients were included in the case group and 8 in the control group. When the survival of pathologically N+ patients was analyzed, both groups showed the same tendency ($P = 0.168$; Fig. 3D).

Table 2. Adverse effects of Bacillus Calmette-Guérin cell wall skeleton treatment

No. of patients	71 (100%)
Nonadverse effect	52 (73)
Adverse effect	19 (27)
Nonmalignant axillary and/or cervical lymph node swelling	9 (13)
ALT and AST elevation (≤grade 2)	6 (8)
Nonmalignant pleural effusion (grade 1)	2 (3)
Infection	1 (1.5)
Neuropathy (grade 2)	1 (1.5)

ALT, alanine aminotransferase; AST, aspartate aminotransferase

Adverse effects were seen in 19 (27%) of the 71 case-group patients (Table 2). These included mild or moderate elevation of alanine aminotransferase and aspartate aminotransferase in six patients, mild nonmalignant pleural effusion in two, and moderate focal infection at the BCG-CWS inoculation site and neuropathy in one patient each. Although there is no grade that refers to the severity of CTCAE, nonmalignant axillary and/or cervical lymph node swelling was observed in nine

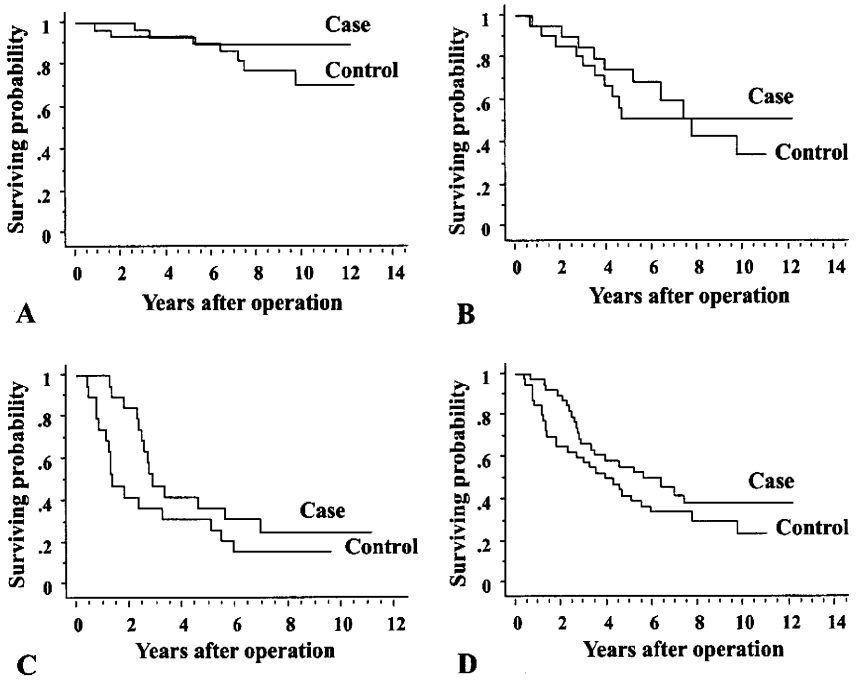

Fig. 3A–D. Kaplan–Meier survival estimates. **A** Stage I. Case-group patients (n = 31) versus controls (n = 31). P = 0.207. **B** Stage II. Case-group patients (n = 21) versus controls (n = 21). P = 0.420. **C** Stage III. Case-group patients (n = 19) versus controls (n = 19). P = 0.114. **D** N(+). Case-group patients (n = 33) versus controls (n = 34). P = 0.168

patients. There was no life-threatening or fatal event. Thirteen of the 19 patients were managed with a temporary dose reduction or discontinuation of BCG-CWS.

Discussion

Immune control of tumor growth can be mediated by the antigen-specific activity of CTLs or by the innate immune response of NK cells. Cytotoxic T cells recognize malignant cells in the context of antigen presentation via major histocompatibility complex (MHC) molecules.[19] Tumor cell recognition by NK cells is antigen-independent and MHC-unrestricted.[20]

Cancer cells share the same MHC as host cells and barely express pathogen-associated molecular patterns (PAMPs). We hypothesized that the inability of tumors to evoke the host immune response is due to the lack of PAMPs in patients with cancer. Supplementation with PAMPs as adjuvants may increase the efficacy of immune responses against tumor antigens (tumor vaccine). Adjuvants are materials added to a vaccine preparation to enhance its immunogenicity. One of the most powerful adjuvants is complete Freund's adjuvant; a suspension of killed mycobacteria in mineral oil. We used BCG-CWS as an adjuvant for this purpose.

Tsuji et al.[8] demonstrated that BCG-CWS can activate immature human dendritic cells (iDC). Antigen presentation and T-cell stimulation are enhanced by BCG-CWS, which also induces up-regulation of the DC maturation marker CD83, and the secretion of inflammatory cytokines such as IL-6, IL-12, and TNF-α. These responses and the increase in antigen-presenting ability indicate that the activation and maturation of DC is induced by CWS-containing mycobacterial peptidoglycan. This suggests that BCG-CWS induces TNF-α secretion from myeloid DC via Toll-like receptor (TLR) 2 and TLR4 and that the secreted TNF-α induces the maturation of DC.

Using a murine subcutaneous and lung metastatic sarcoma treatment model, Mason et al.[21] showed that a local injection of synthetic oligodeoxynucleotides (ODN) containing an unmethylated CpG motif (characteristic of bacterial DNA) could be given with conventional radiation therapy to augment therapeutic efficacy via an apparently immune-mediated mechanism. Combination cancer vaccines with TLR9 agonists such as ODN may induce tumor-specific CD4+ and CD8+ T cells, whose migration and killing activity would be enhanced by radiation therapy. Toll-like receptor expression differences exist between mice and humans; mouse plasmatoid and myeloid DC express TLR9, whereas only human plasmatoid DC does.[22] Mason et al.[21] hypothesized that when radiotherapy is given after TLR agonist injection, the tumor antigens released by dying tumor cells are taken up by activated DC, inducing a tumor-specific T-cell response.

The injection of BCG-CWS sometimes causes lymphadenopathy of the draining lymph nodes (Table 2). We demonstrated the uptake of fluorodeoxyglucose (FDG) into the enlarged lymph nodes not only in the axillary lymph nodes, but also in the cervical and mediastinal lymph nodes by positron emission tomography (PET)

during immunotherapy (data not shown). Lipford et al.[23] reported that among cells within enlarging lymph nodes are many DCs that express increased levels of costimulatory molecules and MHC. Interferon-γ is the final output produced either by the direct stimulation of lymphocytes or by the stimulation of lymphocytes secondary to activation of antigen-presenting cells such as DC. In vitro BCG-CWS induces IL-12 p40 production in peripheral blood culture. Interleukin-12 p40 is an inducible element of IL-12, and in humans may represent IFN-γ-inducing activity.[24]

According to a previous report,[18] BCG-CWS can induce IFN-γ when administered intracutaneously in a patient's upper arm. An elevated serum IFN-γ level is regarded as evidence of a systematic immune response. Interferon-γ is an important immune regulator that performs a wide spectrum of physiologic functions, such as activation of macrophages, NK cells, and CTL, regulation of antigen presentation in many cells, and generation of Type 1 helper T cells (Th1 cells).[25] Our data showed no significant difference in survival between the case-group patients with, and those without IFN-γ induction in the peripheral blood. In this study, we performed IFN-γ assay within 7 months after immunotherapy was started. Matsumoto et al.[24] reported that the levels of production of IFN-γ and IL-10 by lymphocytes were lower in patients with lung cancer than in healthy subjects. In our study, BCG-CWS was repeatedly injected into the skin of both shoulders, for more than 1 year in most patients. When patients receive long-term, repeated inoculations of BCG-CWS, the serum IFN-γ level may increase, especially in those with a good outcome. Our literature search found no report clearly stating an association between increased serum IFN-γ levels and survival benefit in patients receiving BCG-CWS immunotherapy. A recent study of NSCLC patients by Trojan et al.[26] suggested that peritumoral CD8+ T cells exhibit locally higher expression of IFN-γ mRNA; a finding indicative of sustained T-cell reactivity, compared with tumor-infiltrating T lymphocytes (TILs); however, they failed to demonstrate the influence of IFN-γ/CD8 mRNA ratio on overall survival in these patients.

We hypothesized that activation of the innate immune system with BCG-CWS after curative resection for lung cancer may have a survival benefit and conducted a case–control study. Although the difference was not significant, survival of the case-group patients was better than that of the control patients over a long-term follow-up period (Fig. 2). This trend was seen in the subgroups of pathological stage III or lymph node metastasis (Fig. 3C and D). However, there was no difference in survival between the subgroups of p-stage I or II (Fig. 3A and B). These results suggest that monotherapy using BCG-CWS may improve survival without major complications after curative surgery for lung cancer. Patients with advanced lung cancer, especially those with lymph node metastasis, seem to be good candidates for this innate immunotherapy. When patients have micrometastasis to distant lymph nodes, specific cancer antigens may be expressed by the cancer cells and recognized by mature myeloid DC activated with BCG-CWS. The survival benefit of BCG-CWS adjuvant therapy in this series was 17% at 10 years after surgery (Fig. 2A). Tanaka[27] reported a single-institute phase II trial of adjuvant chemotherapy with carboplatin/paclitaxel followed by tegafur and uracil (UFT) for completely resected node-positive (p-stage II-N1 or IIIA-N2) NSCLC. His interim analysis revealed favorable overall and recurrence-free survival of 73% and 49%, respectively, at 3 years, with minimal toxicity. These results suggest that chemotherapy followed by BCG-CWS immunotherapy should be prescribed in a postoperative adjuvant setting after NSCLC resection.

Regarding histological differences between the case and control groups, it was very difficult to completely match three factors at the time of control recruitment. Thus, we gave priority to pathological stage and year of birth. Histology was considered as much as possible but perfectly matched pairing was impossible. According to the survival analysis of BCG-CWS and historical control groups by Yasumoto et al.,[28] all types of lung cancer including squamous cell carcinoma, adenocarcinoma and anaplastic carcinoma were sensitive to treatment with BCG-CWS, and there was no significant difference in survival among those histological types. Their results suggest that the histological differences between case and control group are not of great consequence.

To achieve more effective control of cancer, two modalities should be used with BCG-CWS. The first is the coadministration of a peptide vaccine with BCG-CWS as the adjuvant. The Wilms' tumor gene, *WT1*, is overexpressed in leukemia and a variety of solid tumors, and the WT1 protein has been identified as a tumor-associated antigen.[29] Thus, WT1 products may provide the basis for the development of a new peptide-based anti-cancer immunotherapy. It was demonstrated that 3.0 mg of WT1 therapy can induce a generation of WT1-specific T lymphocytes without damaging normal tissues.[30] Nakajima et al.[31] demonstrated for the first time that a WT1 peptide vaccination combined with BCG-CWS effectively eradicated WT1-expressing tumor cells implanted in mice before vaccination; as a "therapeutic" model, not a "prophylactic" model. Vermorken et al.[32] reported that adjuvant active specific immunotherapy with an autologous tumor cell; namely, BCG (but not CWS) vaccine following surgical resection was more beneficial than resection alone against stage II and III colon cancer. The second modality is the stimulation of NK cells to lyse MHC-unrestricted cancer